Composition and syngeneity of molecular fossils from the 2.78 to 2.45 billion-year-old Mount Bruce Supergroup, Pilbara Craton, Western Australia

JOCHEN J. BROCKS,[1,*] ROGER BUICK,[2] GRAHAM A. LOGAN,[3] and ROGER E. SUMMONS[4]

[1]Department of Organismic and Evolutionary Biology and Department of Planetary and Earth Sciences, Harvard University,
Cambridge, MA 02138, USA
[2]Department of Earth and Space Sciences & Astrobiology Program, University of Washington, Seattle, WA 98195-1310, USA
[3]Geoscience Australia, GPO Box 378, Canberra ACT 2601, Australia
[4]Department of Earth, Atmospheric and Planetary Sciences, Massachusetts Institute of Technology, Cambridge, MA 02139, USA

Abstract—Shales of very low metamorphic grade from the 2.78 to 2.45 billion-year-old (Ga) Mount Bruce Supergroup, Pilbara Craton, Western Australia, were analyzed for solvent extractable hydrocarbons. Samples were collected from ten drill cores and two mines in a sampling area centered in the Hamersley Basin near Wittenoom and ranging 200 km to the southeast, 100 km to the southwest and 70 km to the northwest. Almost all analyzed kerogenous sedimentary rocks yielded solvent extractable organic matter. Concentrations of total saturated hydrocarbons were commonly in the range of 1 to 20 ppm (μg/g rock) but reached maximum values of 1000 ppm. The abundance of aromatic hydrocarbons was ~1 to 30 ppm. Analysis of the extracts by gas chromatography-mass spectrometry (GC-MS) and GC-MS metastable reaction monitoring (MRM) revealed the presence of *n*-alkanes, mid- and end-branched monomethylalkanes, ω-cyclohexylalkanes, acyclic isoprenoids, diamondoids, tri- to pentacyclic terpanes, steranes, aromatic steroids and polyaromatic hydrocarbons. Neither plant biomarkers nor hydrocarbon distributions indicative of Phanerozoic contamination were detected. The host kerogens of the hydrocarbons were depleted in ^{13}C by 2 to 21‰ relative to *n*-alkanes, a pattern typical of, although more extreme than, other Precambrian samples. Acyclic isoprenoids showed carbon isotopic depletion relative to *n*-alkanes and concentrations of 2α-methylhopanes were relatively high, features rarely observed in the Phanerozoic but characteristic of many other Precambrian bitumens. Molecular parameters, including sterane and hopane ratios at their apparent thermal maxima, condensate-like alkane profiles, high mono- and triaromatic steroid maturity parameters, high methyladamantane and methyldiamantane indices and high methylphenanthrene maturity ratios, indicate thermal maturities in the wet-gas generation zone. Additionally, extracts from shales associated with iron ore deposits at Tom Price and Newman have unusual polyaromatic hydrocarbon patterns indicative of pyrolytic dealkylation.

The saturated hydrocarbons and biomarkers in bitumens from the Fortescue and Hamersley Groups are characterized as 'probably syngenetic with their Archean host rock' based on their typical Precambrian molecular and isotopic composition, extreme maturities that appear consistent with the thermal history of the host sediments, the absence of biomarkers diagnostic of Phanerozoic age, the absence of younger petroleum source rocks in the basin and the wide geographic distribution of the samples. Aromatic hydrocarbons detected in shales associated with iron ore deposits at Mt Tom Price and Mt Whaleback are characterized as 'clearly Archean' based on their hypermature composition and covalent bonding to kerogen. *Copyright © 2003 Elsevier Ltd*

1. INTRODUCTION

In a previous paper, we reported the discovery of molecular fossils (biomarkers) in 2.7 billion-year-old (Ga) rocks from a drill core in the Hamersley Basin in Western Australia (Brocks et al., 1999). The extracted bitumens predominantly consisted of *n*-alkanes, methylalkanes and acyclic isoprenoids but also included complex polycyclic biomarkers such as hopanes and steranes. Based on their composition and distribution, the biomarkers were interpreted as indigenous to and syngenetic with their Archean host rocks, thus extending the known biomarker record by > 1 Ga. The biomarkers confirmed the domain Bacteria as an ancient lineage and documented for the first time the existence of eukaryotic organisms in late Archean ecosystems. Hence, if this report is robust, biomarker geochemistry potentially provides a powerful tool for investigating the an-

tiquity and diversity of life on Earth. However, before chemical analysis of solvent-extractable molecules can be adopted as a routine research technique for Archean paleobiology, its integrity must be critically assessed.

The study presented here provides a protocol for the study of hydrocarbon syngeneity in general and for the Archean in particular. It discusses in detail the molecular and carbon isotopic composition and thermal maturity of hydrocarbons extracted from an extended range of late Archean rocks from the Hamersley Basin. Arguments for and against syngeneity are critically assessed, particularly focusing on the possibility that contaminants were introduced during sample preparation and analysis, during drilling and storage, and during post-Archean geological history. It illustrates the level of caution needed before organic geochemical data from extremely old rocks can be accepted as scientifically sound, a skepticism that should be maintained in further work on Archean material. A paleobiological and paleoenvironmental interpretation of the biomark-

* Author to whom correspondence should be addressed (jbrocks@oeb.harvard.edu).

ers is given in a companion paper in this issue (Brocks et al., 2003).

1.1. Precambrian Organic Geochemistry and the Problem of Contamination

Philip H. Abelson was among the first to suggest that the analysis of 'pre-Cambrian fossil biochemicals' might give clues to the evolution of early life (in Woodring, 1954). Subsequently he also detected the first biogenic molecules in Precambrian rocks (in Barghoorn, 1957). In the 1960s a quick succession of reports followed concerning the occurrence of amino acids, fatty acids, porphyrins, *n*-alkanes and acyclic isoprenoids in Precambrian rocks as old as 3.5 Ga. The large number of reports published through the 1960s in the most prominent journals (at least 12 in *Science* and *Nature*) is a good reflection of the enthusiasm sparked by these discoveries (reviews of this early work were given by Hoering, 1967; Rutten, 1971; McKirdy, 1974; Hayes et al., 1983; Imbus and McKirdy, 1993).

However, the syngeneity of saturated hydrocarbons extracted from the metamorphosed Precambrian rocks was questioned at the end of the 1960s and the beginning of the 1970s. The first report dedicated to the problems associated with Precambrian organic trace analyses was by Hoering (1966). He pointed out that the graphitic nature and low hydrogen content of most Precambrian kerogens indicate that the host rock must have had a severe thermal history inconsistent with the survival of soluble organic molecules. Hoering (1966) therefore formulated the rule that extracted alkanes cannot be indigenous unless the pyrolysis of co-occurring kerogen also predominantly yields saturated hydrocarbons. However, pyrolysis experiments on graphitic Precambrian kerogens generally yielded little such material. He then also demonstrated that even Precambrian igneous rocks might yield extractable organic molecules in quantities greatly exceeding the concentrations previously reported for 'Archean' biomarkers. Hoering (1966, 1967) listed a wide range of potential contamination sources: wrapping paper, aluminum foil, laboratory tissue, sample bags, laboratory air and anthropogenic petroleum products that 'appear in unlikely places and could find [their] way into rocks being studied'. Hence, petroleum products of anthropogenic origin might be introduced into Archean rocks during drilling, saw cutting, storage and handling. More obscure but potentially serious sources of contamination may include airborne combustion products, fuel droplets and diesel vapor that could accumulate on samples stored over several years.

In addition, permeability measurements on Archean cherts indicated that contamination might also occur in situ before a rock is drilled and collected (Nagy, 1970; Sanyal et al., 1971). For example, subsurface biologic activity or circulating ground water could have carried biomolecules into the Archean host rocks and a subsequent heating event might then have transformed these biolipids into hydrocarbons. A further source of contamination which is potentially very difficult to distinguish from syngenetic bitumen is petroleum that was expelled from younger source rocks and that penetrated the Archean terrain (first mentioned by Barghoorn et al., 1965, and Meinschein, 1965).

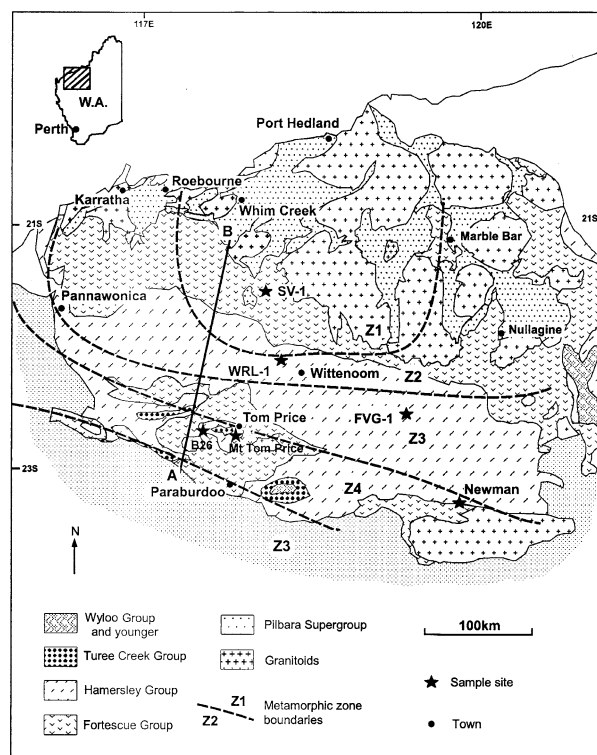The insight that all known early Precambrian rocks are

Fig. 1. Regional geology of the Pilbara Craton, Western Australia. The metamorphic zones Z1 to Z4 refer to burial metamorphic grades of the Fortescue Group (Smith et al., 1982). Z1 = prehnite-pumpellyite zone, Z2 = prehnite-pumpellyite-epidote zone, Z3 = prehnite-pumpellyite-epidote-actinolite zone, Z4 = (prehnite)-epidote-actinolite zone (lower greenschist facies). AB refers to the cross-section in Figure 2.

metamorphosed and the discovery that contamination is a common phenomenon proved daunting and ultimately discouraging. The last papers in the field were published in 1969 (Han and Calvin, 1969; Kvenvolden and Hodgson, 1969; Nagy and Nagy, 1969), and later dissertations on the analysis of organic molecules in Precambrian BIF (Fiebiger, 1973) and Archean stromatolitic carbonates (Wontka, 1979) were never submitted to scientific journals for publication (M. Schidlowski, personal communication). This brief history of Precambrian organic geochemistry thus has a moral: any new report of the discovery of mobile hydrocarbons in Archean rocks must demonstrate syngeneity between molecular fossils and host rock. The molecules reported here and in Brocks et al. (1999) were extracted from rocks that are > 1 Ga older than the previously oldest accepted bitumen from the 1.64-Ga Barney Creek Formation, Northern Territory (Summons et al., 1988). Therefore arguments for and against the different sources of contamination are considered here in detail. The data and its syngeneity status will form the basis for further interpretation in other publications of this series.

1.2. Geological Setting and Samples

The Archean Pilbara Craton is exposed over an area of ~180,000 km² in the northwest of Western Australia (Fig. 1) and comprises a 3.5-Ga (Buick et al., 1995) to 2.85-Ga

(Krapez, 1993) granitoid-greenstone basement (Pilbara Supergroup) cropping out over an area of 60,000 km². After cratonization, the volcano-sedimentary Mt Bruce Supergroup was deposited in the Hamersley Basin between 2.78 and 2.45 Ga (Arndt et al., 1991; Barley et al., 1997). The Mt Bruce Supergroup, subdivided into the Fortescue, Hamersley and Turee Creek Groups, has a maximum thickness of 6.5 km and an outcrop area of ~100,000 km². The margins of the craton to the south are covered by the Paleoproterozoic Wyloo Group and younger Proterozoic successions, and to the east and west by Phanerozoic deposits of the Canning and Carnarvon Basins, respectively. Both Phanerozoic basins are oil producers. In the Carnarvon Basin large volumes of petroleum are sourced and produced mostly offshore from Mesozoic sediments (Bradshaw et al., 1994). In the onshore Canning Basin, marginally economic volumes of hydrocarbons have been sourced from Ordovician to Permian sediments. The volumes of Canning hydrocarbons may have been much larger in the past since hydrocarbon generation in this basin took place before Triassic times with many accumulations lost during subsequent tectonism, especially during the Late Triassic Fitzroy Movement (Kennard et al., 1994). However, all oil sources are at least a hundred kilometers from the nearest exposures of the Mt Bruce Supergroup.

A short lithostratigraphic description of the relevant formations of the Fortescue Group and Hamersley Group and information about their depositional setting is provided in the Appendix. Details of sample locations and lithologies are summarized in Table 1. Samples were collected from diamond drill core or from mine benches to limit surficial contamination and the effects of modern oxidative weathering. Both highly kerogenous and non-kerogenous rocks were collected from the same sites, the latter acting as a control for contamination. Where possible, samples were deliberately selected from the least deformed and metamorphosed parts of the craton.

1.3. Regional Metamorphism and Structural Deformation of the Hamersley Basin

Both the Pilbara basement and the overlying rocks of the Hamersley Basin are generally characterized by exceptionally low metamorphic grades for their age (Smith et al., 1982), coupled in many areas with minimal deformation. The southern margin of the Hamersley Basin was deformed as a part of a foreland fold-and-thrust belt during collision with the Yilgarn craton 2.3 to 2.2 Ga ago (Opthalmian Orogeny) and during Capricorn orogenesis between 1.82 and 1.65 Ga (Harmsworth et al., 1990; Martin et al., 1998). As a result, the supracrustal rocks of the Mount Bruce Supergroup are now regionally folded into an east-west trending synclinorium. The northern part of the Basin dips gently to the south (5–10°) and the area immediately south of the synclinorial axis dips gently to the north. Folding increases in intensity further southward, but schistosity and cleavage only become conspicuous close to the southern basin margin (Smith et al., 1982). The samples studied here have undergone only minimal deformation, except those from Newman.

Burial metamorphism of the Fortescue and Hamersley Group was initiated by deposition of the Paleoproterozoic Turee Creek

Group and Wyloo Group, which dominantly occurred in the southern part of the basin (Martin et al., 1998). Smith et al. (1982) defined four metamorphic zones for the Mount Bruce Supergroup based on mineral assemblages in metabasic rocks of the Fortescue Group (basalts, andesites and their pyroclastic equivalents). Rocks with the mildest thermal history (Zone I) are characterized by prehnite and pumpellyite, Zone II by prehnite-pumpellyite-epidote, Zone III by prehnite-pumpellyite-epidote-actinolite and Zone IV by (prehnite)-epidote-actinolite. Zone I and II belong to the prehnite-pumpellyite facies, Zone III the prehnite-actinolite facies and Zone IV the lower greenschist facies (Smith et al., 1982). However, the temperatures responsible for generating these mineral assemblages are poorly constrained. Smith et al. (1982) estimated 100 to 300°C for Zones I and II, and 300 to 360°C for Zone III. Frey et al. (1991) restricted the P-T stability field for prehnite-pumpellyite to 175 to 280°C (0.5–4.5 kbar) and for prehnite-actinolite to 220 to 320°C (<4.5 kbar). The transition from subgreenschist to greenschist facies occurs between 250 and 300°C (<2–4 kbar) (Frey et al., 1991).

The regional distribution of the four metamorphic zones in the Fortescue Group is illustrated in Figure 1. The grade of metamorphism increases towards the south (Smith et al., 1982), caused by burial under an increasing load of Proterozoic cover (Fig. 2). As suitable rock types for metamorphic assessment are absent from the Hamersley Group, the zone boundaries in Figure 1 exclusively refer to the Fortescue Group. However, metamorphic grades of the overlying Hamersley Group can be roughly determined by extrapolation of estimated temperature gradients to shallower burial depths (Fig. 2). Hence, inferred regional metamorphic grades for locations where samples were collected are summarized in Table 2. It is likely that all samples have undergone regional metamorphism below greenschist facies. However, it is possible that the thermal history of some samples has been complicated by unrecognized local heating events resulting from hydrothermal activity or igneous intrusions (Barley et al., 1999). A generally mild thermal history overprinted by local heating events is also reflected by kerogen reflectance data (R_o) from shales from the iron ore mine at Mt Tom Price (Taylor et al., 2001). At Mt Tom Price, shales from the Mt McRae Shale below the orebody footwall zone and shales from the Brockman Iron Formation above the footwall zone have average R_o = 2.5 to 2.7% with minima at ~2.0%, consistent with the preservation of saturated hydrocarbons. However, within 10 m of the footwall zone R_o reaches values of up to 7% suggesting maximum temperatures beyond the stability field of organic molecules.

The timing of peak metamorphism in the Hamersley Basin has been dated by several different isotopic systems on several different metamorphic minerals. All yield reasonably consistent dates between ~2.3 and ~2.0 Ga. The most relevant for this study comes from metamorphic monazite from the Roy Hill Shale in WRL-1, which yields a U-Pb age of 2192 ± 5 Ma (Rasmussen et al., 2001). As this evidently records a thermal event associated with hydrothermal activity in the nearby Mt Tom Price iron mine, it probably represents the age of the most profound metamorphic modification of the Hamersley Basin bitumens.

Table 1. Bulk characteristics and extract yields.

Sample	Formation or member	Well	Depth (m)	Lithology	Mass[a] (g)
Hamersley Group					
Tom Price area					
Dal1	Dales Gorge Mm	DE20/74	350.30	Dark gray chloritic mudstone	119.5
Dal2*	Dales Gorge Mm	G1185-81	269.03	Finely plane-laminated BIF	100
Rae1	Mt McRae Shale	G1185-81	324.87	Massive siliceous black kerogenous mudstone	81.2
Rae2	Mt McRae Shale	B26-7	140.75	Massive soft black shale	100
Rae6	Mt McRae Shale	Mine	—	Plane-laminated black shale; hematite; pyrite	110.4
Bee1	Mt McRae Shale	G906	418.90	Massive black kerogenous mudstone	112.6
Mt Whaleback Mine					
Wal2	Whaleback Mm	DDH257	48.9	Dark gray kerogenous shale	25.1
Rae3	Mt McRae Shale	Mine	—	Weakly plane laminated black shale	120
Rae5	Mt McRae Shale	DDH324	139.7	Deep-black highly kerogenous shale	13
Wittenoom					
Wal1*	Whaleback Mm	DDH47A	256.7	Medium gray kerogen-poor shale	25.2
Rae4*	Mt McRae Shale	DDH47A	397.7	Light gray kerogen-free shale	30
Mam3*	McLeod Mm	WRL-1	581.17	Light to medium gray mudstone	125
Mam2	Nammuldi Mm	WRL-1	644.50	Plane-laminated black mudstone	94.2
Mam1	Nammuldi Mm	WRL-1	665.39	Sideritic dark brown mudstone	80.2
Fortescue Group					
Roy1	Roy Hill Shale	WRL-1	679.39	Siliceous, pyritic black shale	105
Roy10	Roy Hill Shale	WRL-1	679.94	Siliceous, pyritic black shale	114.6
Roy2	Roy Hill Shale	WRL-1	681.69	Siliceous, pyritic black shale	71
Roy11	Roy Hill Shale	WRL-1	695.75	Siliceous, pyritic black shale	101.2
Roy3	Roy Hill Shale	WRL-1	718.07	Siliceous, pyritic black shale	95.5
War5	Warrie Mm	WRL-1	741.94	Siliceous, pyritic black shale	107.9
War1*	Warrie Mm	WRL-1	777.86	Massive black chert	149.2
Mad1*	Maddina Basalt	WRL-1	780.51	Medium gray amygdaloidal basalt	48.5
Har1	Hardey Fm[f]	WRL-1	1824.3	Dark gray silty shale; 1cm pyrite nodules	95
FVG1	Rov Hill Shale	FVG-I	756.04	Weathered and fractured black shale	109.9
FVG2	Warrie Mm?	FVG-I	860.15	Weathered and fractured gray silty mudstone	100
War2	Warrie Mm	Surface	—	Compact dark gray shale	145.1
Tum1	Tumbiana Fm	SV-I	115.02	Pyritic black kerogenous mudstone	100.0

[a] Mass of solvent extracted rock powder.

[b] Total organic carbon, here defined as % kerogen of total rock mass (the generally low bitumen content was neglected).

[c] Sat = saturated hydrocarbon fraction; Aro = aromatic fraction; 1ppm = 1 μg hydrocarbons per gram of rock. Quantification was by GC-FID using internal standards as described in section 2.5. (accuracy ±20%). Values differ from Brocks et al. (1999) where reported extract yields are gravimetric.

[d] n-C^{max} is the most abundant n-alkane (given in brackets).

[e] Estimated by GC-MS MRM with D_4 as internal standard and as described in section 2.5. Steranes = ΣC_{27} to C_{29} $\alpha\alpha\alpha$ and $\alpha\beta\beta$-steranes and $\beta\alpha$-diasteranes; Hopanes = Σ Ts, Tm, C_{29}-$\alpha\beta$, C_{29}Ts, C_{30}-$\alpha\beta$, C_{31}-$\alpha\beta$-22 (S + R), C_{31}-2α-Me (compound abbreviations are defined in the text).

[f] Langwell Creek Sequence below the Lyre Creek Agglomerate Member.

* = Kerogen-free or kerogen-poor control sample (blank sample); '—' = not detectable; " = not measured.

1.4. The Thermal Stability of Hydrocarbons Under Geological Conditions

Although the samples are undeformed and extremely well preserved by Archean standards, they have still suffered lowest grade metamorphism, probably corresponding to temperatures between 200 and 300°C. Can C_{15+} hydrocarbons survive these extreme conditions? Unfortunately, the boundary parameters for the preservation of organic molecules under geological conditions are not well constrained (Price, 1997). However, it is possible to obtain reliable information on lower limits of molecular preservation by observing deep-subsurface petroleum reservoirs that exist at exceptionally high present day temperatures. Pepper and Dodd (1995) described petroleum reservoirs in Triassic to Middle Jurassic sandstones of the Central Graben, North Sea, where oil and condensate exist at accurately measured present day temperatures of 120 to 195°C. Despite the high temperatures, n-alkanes with > 35 carbon atoms, and sterane and hopane biomarkers are preserved even

in the hottest pools. The Elgin and Franklin fields in the North Sea off Scotland are commercially exploited high temperature oil reservoirs located at > 5.2 km depth (Knott, 1999). The temperature of the oil in the subsurface is 185°C in Elgin and 196°C in Franklin, with reservoir pressures exceeding 1000 bar. Brigaud (1998) even reported a maximum temperature of 203°C within the Franklin field. Another example of a high temperature petroleum field is Sweethome in South Texas (McNeil and BeMent, 1996). The reservoir produces gas condensate at present day temperatures of up to 200°C. Despite the fact that the reservoir has been at maximum temperature for a period of 30 Ma, hopane biomarkers with up to 35 carbon atoms are apparently still preserved. An even higher temperature, 208°C, was measured for an oil reservoir in Hungary at 4.8 km depth (Sajgó, 2000). Moreover, relatively immature to moderately mature kerogens and bitumens were detected in the rapidly subsiding Los Angeles Basin at present day temperatures of up to 223°C (Price, 2000).

Sample	TOC (%)[b]	Sat[c] (ppm)	Aro[c] (ppm)	Sat/Aro	n-C^{max} (ppm)[d]	Pr/Ph	Pr/n-C$_{17}$	Ph/n-C$_{18}$	Steranes (ppb)[c]	Hopanes (ppb)[c]
Hamersley Group										
Tom Price area										
Dal1	1.3	74	8.7	8.5	2.3 (C$_{14}$)	2.0	0.42	0.29	6.6	8.2
Dal2	0.0	0.4	0.02	20	0.002 (C$_{23}$)	—	—	0.36	0.71	1.0
Rae1	5.8	440	27	16	11 (C$_{11}$)	2.2	0.40	0.23	17.3	8.9
Rae2	6.0	1000	8.8	110	34 (C$_{11}$)	2.6	0.61	0.41	23.3	16.7
Rae6	7.2	0.06	13	0.005	—	—	—	—	—	—
Bee1	7.8	120	16	7.5	3.3 (C$_{11}$)	2.6	0.60	0.30	10.6	19.0
Mt Whaleback Mine										
Wal2	2.5	110	17	6.5	8.8 (C$_{12}$)	2.7	0.58	0.35	52	35
Rae3	5.3	2.1	0.03	70	0.03 (C$_{16}$)	1.9	0.82	0.69	0.24	0.16
Rae5	7.9	86	17	5.1	4.1 (C$_{14}$)	1.9	0.58	0.20	9.7	14.2
Wittenoom										
Wal1*	0.6	7.3	1.1	6.6	0.86 (C$_{14}$)	1.3	0.46	0.11		
Rae4*	0.0	0.9	0.07	13	0.21 (C$_{14}$)	—	—	—	0.55	1.0
Mam3*	0.0	0.8	0.2	4.0	0.06 (C$_{22}$)	—	—	—	1.5	2.4
Mam2	2.7	1.3	0.8	1.6	0.005 (C$_{16}$)	1.7	0.29	0.24	3.7	5.6
Mam1	2.6	13	2.6	5.0	0.83 (C$_{18}$)	1.1	0.18	0.11	6.1	8.0
Fortescu Group										
Roy1	7.4	20	1.5	13	0.80 (C$_{19}$)	1.2	0.31	0.20	9.9	10.7
Roy10	3.7	9.4	1.7	5.5	0.20 (C$_{11}$)	1.9	0.33	0.21	7.0	6.0
Roy2	8.6	18	0.00	—	0.60 (C$_{18}$)	1.3	0.41	0.27	4.9	2.0
Roy11	11.4	15	3.5	4.3	0.14 (C$_{12}$)	1.4	0.30	0.24	11.7	9.7
Roy3	9.0	13	2.5	5.2	0.42 (C$_{18}$)	1.4	0.33	0.20	4.0	3.6
War5	6.9	2.2	1.0	2.2	0.055 (C$_{13}$)	1.6	0.41	0.39	2.7	2.6
War1*0.5	—	—	—	—		—	—	0.27	0.39	
Mad1*	0.0	0.1	0.00	—	0.004 (C$_{22}$)	—	—	—	0.13	0.17
Har1	1.6	5.2	1.1	4.7	0.17 (C$_{16}$)	4.0	0.44	0.16	1.9	1.9
FVG1	9.4	2.0	0.7	2.9	0.21 (C$_{19}$)	1.4	0.41	0.39	9.6	9.9
FVG2	1.5	0.9	0.08	11	0.02 (C$_{16}$)	2.1	0.45	0.22	1.7	2.1
War2	1.3	0.04	0.01	4	0.0007 (C$_{20}$)	—	—	—	0.09	0.09
Tum1	0.9	0.7	0.06	12	0.02 (C$_{18}$)	1.7	0.36	0.18	0.33	0.85

The existence of these high temperature reservoirs and source rocks proves that high molecular weight hydrocarbons can survive for geological periods of time at temperatures clearly above 200°C. This observation agrees with kinetic models of oil degradation that predict persistence of bitumen to ~250°C (Pepper and Dodd, 1995; Burnham et al., 1997; Dominé et al., 2002). Therefore, the thermal history of the best preserved Archean rocks (200–300°C) is potentially consistent with the existence of indigenous C$_{15+}$ hydrocarbons.

2. EXPERIMENTAL

2.1. Solvents and Materials

n-Hexane (Waters; LC-grade) was distilled twice and methanol (BDH; HiperSolv) distilled once before use. Dichloromethane (DCM) (Mallinckrodt; UltimaAR) was used without further purification. All solvents were tested for purity by concentrating 100 to 0.1 mL and analyzing by GC-FID as described below. Glass wool and aluminum foil were combusted at 400°C for 16 h and quartz sand at 900°C for 24 h. Glassware was cleaned with Extran AP 11 (Merck), rinsed twice with distilled water and annealed at 350 to 450°C in a ventilated oven for 16 h. Septa for sample-vials (red TFE/silicone; Alltech) were rinsed with DCM twice. Tools used to prepare rock samples were cleaned with hot tap water and rinsed with distilled water, methanol and DCM.

2.2. Sample Preparation

Samples were processed in batches of six, commonly including one kerogen-free sample ('blank-rock') and one procedural blank. To reduce the impact of cross-contamination, all steps from sample cleaning and crushing to extraction and fractionation were performed in the same sample order, starting with the least kerogenous rock and ending with the most kerogenous. The procedural blank was processed between the second to fifth sample. Dust was removed from rock samples by water washing and then ultrasonication in distilled water for ~10 s. Potential organic contaminations adsorbed to rock surfaces were analyzed by the slice-extraction technique (Brocks, 2001). The rock was ground to <200 mesh grain size in a ring-mill. The mill was cleaned between samples by water washing and then by grinding annealed quartz sand two to three times for 60 s.

Twenty-five to 150 g of the rock powder were extracted for 72 h with 350 mL DCM in a Soxhlet apparatus fitted with an annealed glass
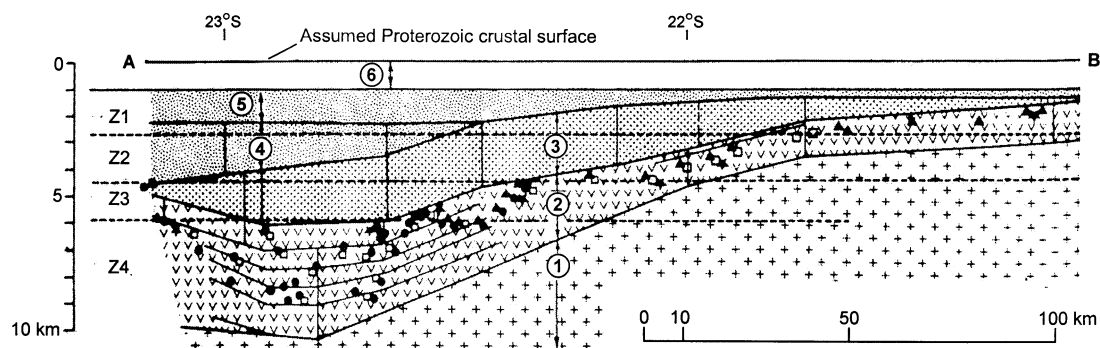
Fig. 2. Reconstructed unfolded cross-section along AB in Figure 1. Z1 to Z4 refer to the metamorphic zones. Units are: 1 = Archean basement, 2 = Fortescue Group, 3 = Hamersley Group, 4 = present Turee Creek Group, 5 = assumed original thickness of Turee Creek Group, 6 = assumed additional Proterozoic cover. Circles, triangles and squares refer to sites where samples for the analysis of metamorphic minerals were collected (Smith et al., 1982). Modified after Figure 3 in Smith et al. (1982) by permission of Oxford University Press.

microfibre thimble (Whatman). Samples < 25 g were placed in glass containers, covered with aluminum foil and ultrasonicated in 20 mL DCM for 10 min, then five times in 10 mL DCM for 3 min. Combined extracts were reduced to 10 mL in a clean rotary evaporator at 600 mbar and further reduced to 4 mL under a stream of purified nitrogen gas. The concentrate was then centrifuged for 5 min at 2000 rpm in a closed 4-mL vial to remove suspended rock particles. Twenty percent of the extract was removed and further reduced to 100 μL for analysis as EOM (unfractionated 'extracted organic matter'). The remaining extracts were separated into saturated, aromatic and polar fractions by liquid chromatography on glass columns (6 mm i.d.) dry-packed with 1.4-g silica gel. Silica gel (Silica Gel 60; grain size 0.063–0.200 mm; Merck) was heated at 400°C for 24 h and deactivated with 2% distilled, n-hexane-extracted water. The extracts in 50 μL DCM were transferred to the top of the column in fractions of five times 10 μL and dried at room temperature between each transfer. Saturated hydrocarbons were eluted with n-hexane (4 mL), aromatic hydrocarbons with n-hexane:DCM (1:1 v/v, 4 mL) and polars with DCM:methanol (1:1 v/v, 4 mL). The solvents were reduced to 100 μL in a stream of nitrogen. Sulfur in the saturated fraction was removed by filtration over freshly precipitated elemental copper.

Added as internal standards to the saturated hydrocarbon fraction were aC_{22} (3-methylhenicosane, 99+% purity; ULTRA Scientific) and D_4 (d_4-C_{29}-$\alpha\alpha\alpha$-ethylcholestane; Chiron Laboratories AS), and to the aromatic hydocarbon fraction D_{14} (d_{14}-$para$-terphenyl, 98 atom% deuterium; Aldrich Chem. Co.).

2.3. Instrumental Analyses

2.3.1. Bulk characteristics

Kerogen contents (~TOC) and ROCK-EVAL parameters were determined on a VINCI ROCK-EVAL 6 instrument according to established procedures (Espitalié et al., 1977).

2.3.2. Gas chromatography (GC)

GC analyses were performed using a Hewlett Packard HP6890 gas chromatograph fitted with a flame ionization detector (FID) and a HP Ultra 1 column (25 m × 0.25 mm i.d., 0.33 μm film thickness) using manual injection in splitless mode and H_2 as carrier gas. The oven was programmed at 40°C (2 min) and heated to 310°C at 4°C/min, with a final hold time of 15 min.

2.3.3. Gas Chromatography-Mass spectroscopy (GC-MS)

GC-MS analyses in the full-scan mode and by selected ion recording (SIR) were carried out on a VG AutoSpecQ and a Hewlett Packard 5973 Mass Selective Detector (MSD). The AutoSpecQ was equipped with a Fisons GC 8000 Series gas chromatograph and a DB-5 coated capillary column (60 m × 0.25 mm i.d., 0.25 μm film thickness) using H_2 as carrier gas. Samples were injected in splitless mode or on-column. The GC oven was programmed at 60°C (2 min), heated to 310°C at 4°C/min, with a final hold time of 25 min. The source was operated in EI-mode at 70 eV ionization energy. The AutoSpec full-scan rate was 0.40 s/decade over a mass range of 50 to 500 Da and a delay of 0.20 s/decade. Data were acquired and processed using OPUS V3.6X (Fisons Instruments). The HP 5973 MSD was equipped with a HP6890 gas chromatograph (Hewlett Packard) and a HP-5 coated column (50 m × 0.20 mm i.d., 0.11 μm film thickness). Samples were injected in pulsed splitless mode with He as carrier gas. The GC oven was programmed at 40°C (2 min), heated to 310°C at 4°C/min and held at the maximum temperature for 25 min. The MS source was operated in EI-mode at 70 eV.

2.3.4. Metastable reaction monitoring (GC-MS MRM)

Biomarkers were analyzed by GC-MS MRM on a VG AutoSpecQ with the same GC conditions as described for SIR experiments. The

Table 2. Regional metamorphic grades for sample locations in the Pilbara Craton determined from Smith et al. (1982).

Sample location or well[a]	Formations	Zone[b]
SV-1	Tumbiana Fm (Fortescue Group)	Zone I–II
WRL-1	Marra Mamba Iron Fm (Hamersley Group) to Hardey Fm (Fortescue Group)	Zones I–II
Tom Price	Mt McRae Shale to Brockman Iron Fm (Hamersley Group)	Zone II–III
Newman	Mt McRae Shale to Brockman Iron Fm (Hamersley Group)	Zone II–III
FVG-I	Jeerinah Fm (Fortescue Group)	Zone III

[a] See Figure 1.
[b] Zone I = prehnite-pumpellyite zone; Zone II = prehnite-pumpellyite-epidote zone; Zone III = prehnite-pumpellyite-epidote-actinolite zone.

source was operated in EI-mode at 250°C, 70 eV ionization energy and 8000 kV acceleration voltage. Di- to pentacyclic terpanes and steranes were measured in parent to daughter (123, 177, 191, 205, 217, 231, 245 Da) transitions with cycle times of 1.4 to 2.1s.

2.4. Isotopic Analyses

The stable carbon isotopic composition of kerogen was determined according to standard sealed tube combustion techniques (Sofer, 1980).

The carbon isotopic composition of individual hydrocarbons was determined by gas chromatography-isotopic ratio mass spectroscopy (GC-IRMS). The analytical system included a Varian 3400 GC connected to a CuO/Pt combustion unit interfaced to a Finnigan MAT 252 isotope-ratio mass spectrometer. Samples were manually injected on-column and the programmable GC injector was immediately ramped from 60 to 300°C at 150°C/min and held at the final temperature for 8.4 min. Helium was used as the carrier gas and the GC capillary column was a DB-1 (60 m × 0.25 mm i.d., 0.25 μm film thickness). The GC oven was programmed at 40°C for 10 min, heated to 310°C at 4°C/min and held at the final temperature for up to 10 min. Better resolution was obtained for pristane and phytane by reducing the heating rate to 2°C/min. Data was acquired and processed using the software package ISODAT version 7. The system was calibrated by co-injecting perdeuterated n-alkanes (Chevron) with known isotopic composition. Statistical errors are reported in Appendix B, Table A4. All $\delta^{13}C$ values are reported relative to PDB.

2.5. Quantification

Total yields of extracted saturated and aromatic hydrocarbons in ppm (μg per gram of rock) were determined by integration of total GC-FID signals and using aC_{22} and D_{14} internal standards (maximum 20% variation in repeat-analyses). Values obtained this way were 30 to 50% lower than data previously reported based on gravimetric analyses (Brocks et al., 1999). The latter method was avoided because solvent removal causes loss of lighter hydrocarbons and residual solvent in bitumen causes large systematic errors for samples in the submilligram range.

Absolute concentrations of n-alkanes were determined by integration of corrected GC-FID or GC-MS $m/z = 85$ signals using aC_{22} as the internal standard. Absolute quantities determined by GC-FID and GC-MS were within ~10%. Aromatic hydrocarbons were quantified relative to D_{14} using GC-MS partial ion chromatograms of the parent ion recorded in full scan or SIR mode. Signal areas were corrected using response factors determined by injection of defined concentrations of commercially available standards. Absolute concentrations of sterane and hopane biomarkers were estimated by GC-MS MRM with D_4 as the internal standard. Uncorrected signal areas of steranes were determined in $M^+ \rightarrow 217$ transitions, hopanes in $M^+ \rightarrow 191$ transitions, A-ring methylated hopanes in $M^+ \rightarrow 205$ transitions, and the standard D_4 in the $404 \rightarrow 221$ transition.

3. RESULTS AND DISCUSSION

3.1. Bulk Characteristics and Extract Yields

Bulk characteristics and solvent extract yields are summarized in Table 1. The analyzed samples have a wide variety of lithologies and kerogen contents, ranging from kerogen-free mudstones, BIF and basalt, to kerogen-rich black shales with up to 11% total organic carbon (TOC). The Mt McRae Shale from the Hamersley Group in the Tom Price area contains highly mature kerogen with H/C ratios of ~0.1 (Hayes et al., 1983), and kerogens from drill core WRL-1 from the Wittenoom area have H/C ≈ 0.1 to 0.3 (R. Buick, unpublished results). The hydrogen contents of the kerogens were generally too low to obtain reliable ROCK EVAL data ($T_{max} \sim 500°C$ or higher, hydrogen index HI ≈ 0).

The yields of hydrocarbons obtained by Soxhlet extraction of rock powder with dichloromethane were generally low. Sam-

ples with low kerogen contents (TOC < 1%) yielded < 1 ppm and kerogen-rich shales up to 1000 ppm (Table 1). Yields of saturated hydrocarbons from shales of the Hamersley Group from the Tom Price and Newman areas show large variations even for kerogen rich samples. For example, Mt McRae Shale sample *Rae3* (5.3% TOC) contains 2.1 ppm saturated hydrocarbons while *Rae2* (6.0% TOC) yielded 1000 ppm. Concentrations of aromatic hydrocarbons in the Mt McRae Shale vary from 0.03 to 27 ppm. Hydrocarbon concentrations in samples from the Fortescue Group were commonly lower than in the Hamersley Group. The absolute concentrations of hopane and sterane biomarkers are low in all samples, ranging from 0.1 to 20 ppb (nanograms per gram of rock) (Table 1). Biomarker concentrations <1 ppb were not considered to be reliable and were not used to interpret samples.

3.2. Bitumen Composition

3.2.1. Normal-, Branched- and Cyclohexylalkanes

Most samples from the Hamersley and Fortescue Groups have condensate-like n-alkane distributions (Fig. 3). The highest molecular weight (MW) n-alkanes resolved under GC conditions are n-C_{19} to n-C_{23} in all samples from drill core WRL-1 and in all black shales from Mt Tom Price and Mt Whaleback. In most kerogen-rich samples, n-alkanes with low carbon numbers (n-C_9–n-C_{12}) are the most abundant components (hydrocarbons < n-C_9 were not recovered by the extraction procedure). Kerogen is a strong adsorbent for hydrocarbons (Oehler, 1977) and high kerogen contents protect compounds with low molecular mass against expulsion and evaporation. Thus, in kerogen-poor Pilbara samples light hydrocarbons are generally depleted and the n-alkane range shifts towards higher molecular masses (e.g., samples *Dal1* and *Tum1* in Fig. 3). Preferences for n-alkanes with odd or even numbers of carbon atoms were not observed.

Monomethylalkanes (Fig. 4), were detected in all samples over the same carbon-number range as n-alkanes. Isomers with all possible branching positions were identified in similar concentrations and no predominance of end- or midbranched monomethylalkanes was detected.

N-alkylcyclohexanes, visible in substracted $m/z = 83$ to 85 chromatograms (Fig. 4C), were detected in all samples in low relative concentrations and occurred over the same MW range as the n-alkanes (Fig. 4). The acyclic isoprenoids pristane (Pr) and phytane (Ph) are abundant in all bitumens (Figs. 3 and 4B). The Pr/Ph ratio in samples from the Fortescue Group lies consistently between 1 and 2 (except in *Har1* from drill core WRL-1), while bitumens of the Hamersley Group have marginally higher Pr/Ph ratios (2.0–2.7) and slightly increased values for the Pr/n-C_{17} and Ph/n-C_{18} ratios (Table 1). Acyclic isoprenoids with ≤ 18 carbon atoms (except for 17) also occur in all samples in concentrations similar to Pr and Ph (Fig. 4), while pseudohomologues with 17 and > 20 carbons atoms were not detected.

Unresolved complex mixtures (UCMs or 'humps') underlying the n-alkanes have low concentrations in most samples (Fig. 3). A slightly increased UCM in *Rae3* (Fig. 3), a mine-bench sample from Mt Whaleback, is probably caused by biodegradation, an interpretation supported by higher Pr/n-C_{17}
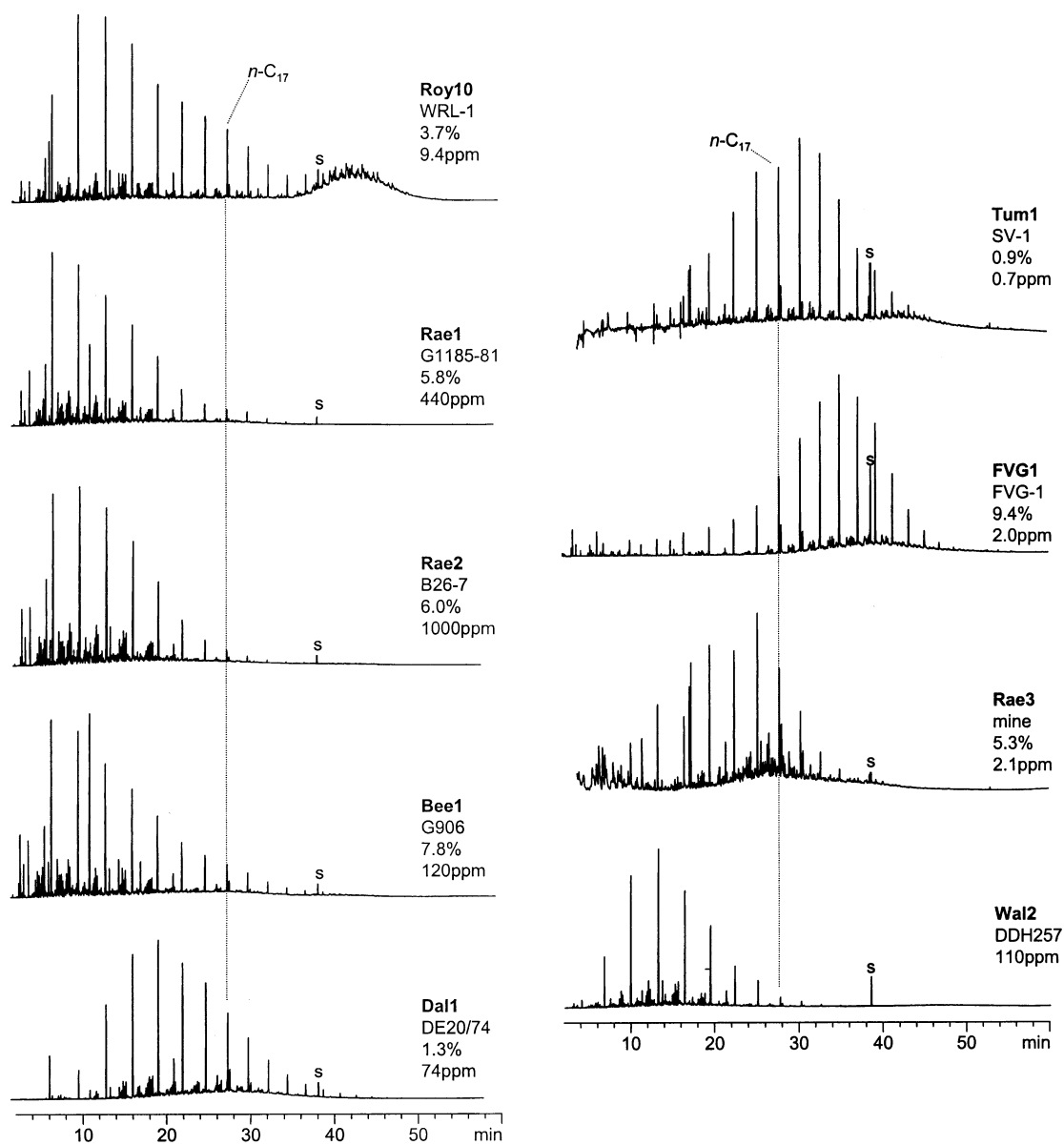
Fig. 3. Gas chromatograms of saturated hydrocarbons in bitumens from the Fortescue and Hamersley Groups. The chromatograms are identified by sample name, drill core, kerogen content (TOC) and extract yield of the saturated hydrocarbon fraction in ppm. 's' is the internal standard. The dotted line marks n-heptadecane.

and Ph/n-C$_{18}$ ratios in this sample (Table 1). An unusual UCM at high retention times was detected in all samples from drill core WRL-1 (Fig. 3).

3.2.2. Adamantanes and Diamantanes

Adamantane and diamantane and their methylated homologs occur only in low relative concentrations in the Fortescue Group and lower Hamersley Group (<0.01 μg/g rock; in procedural blanks adamantanes and diamantanes were always below the detection limit). However, in bitumens from the Hamersley Group at Mt Tom Price and Mt Whaleback they are one to two orders of magnitude more abundant than in the Fortescue Group. In Mt McRae Shale sample *Rae6* from Mt Tom

Price, adamantanes (0.027 μg/g) and diamantanes (0.038 μg/g) are even the sole constituents of the saturated hydrocarbon fraction. Adamantanes and diamantanes are discussed in more detail in section 3.4.2.

3.2.3. Cheilanthanes

GC-MS metastable reaction monitoring (MRM) of m/z = 191 daughter ions in the C$_{19}$ to C$_{25}$-range of tricyclic terpanes revealed the presence of 13β(H),14α(H)-cheilanthanes in all samples (Fig. 5), but in different distributions. C$_{23}$ is the most abundant homologue in all bitumens from the upper Fortescue Group, while C$_{19}$ to C$_{22}$-homologues have very low relative abundances (Fig. 5A). In contrast, all bitumens from
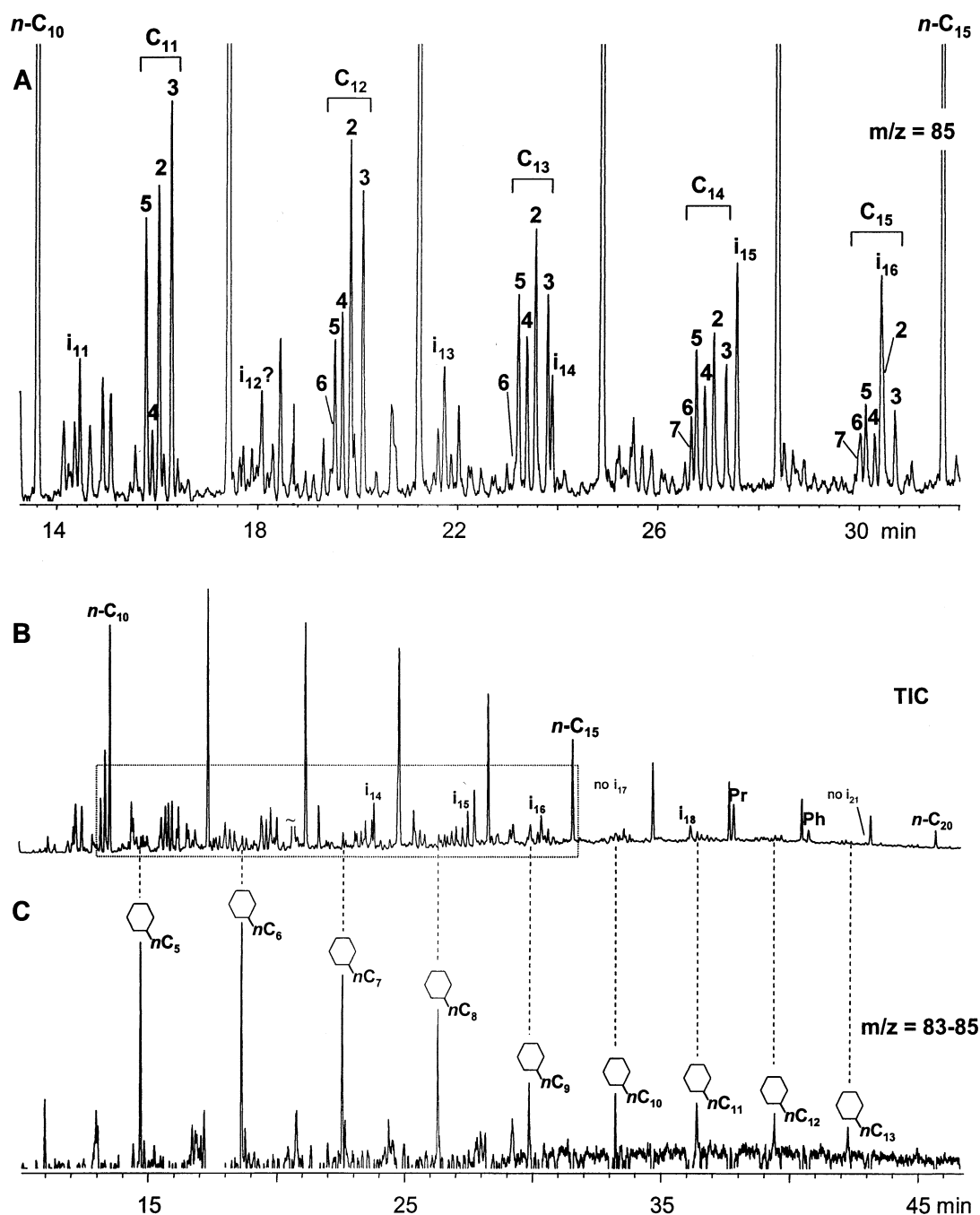
Fig. 4. Mass-chromatograms of saturated hydrocarbons in Mt McRae Shale *Bee1*. (A) Mass-chromatogram m/z = 85 showing methylalkanes and acyclic isoprenoids. Monomethylalkanes are identified by carbon number (C_{11}, C_{12} etc.) and branching position. Acyclic isoprenoids are identified by carbon number (i_{13}–i_{18}; referring to 2,6,10-trimethyl substituted alkanes; Pr [pristine] = i_{19}; Ph [phytane] = i_{20}). Note that signal areas in m/z = 85 mass-chromatograms are not proportional to compound concentrations leading, for example, to a reduced response in 4-methylalkanes. (B) Total ion current (TIC). '~' = Indicates truncated naphthalene signal. (C) Mass-chromatogram m/z = 83 minus 85 showing *n*-alkylcyclohexanes.

the Hamersley Group at Mt Tom Price have high relative concentrations of the C_{19} to C_{21}-homologues (Fig. 5B). While such a difference in the distribution of cheilanthanes could be the result of a change in their biologic source, other observations do not support this suggestion. The positions of the UCMs

underlying the tricyclic terpanes in the reconstructed MRM chromatograms indicate a general bias towards high MW tricyclic hydrocarbons in Fortescue Group samples (Fig. 5A) and to lighter molecular masses in Hamersley Group samples (Fig. 5B). The average molecular mass of UCMs is probably a
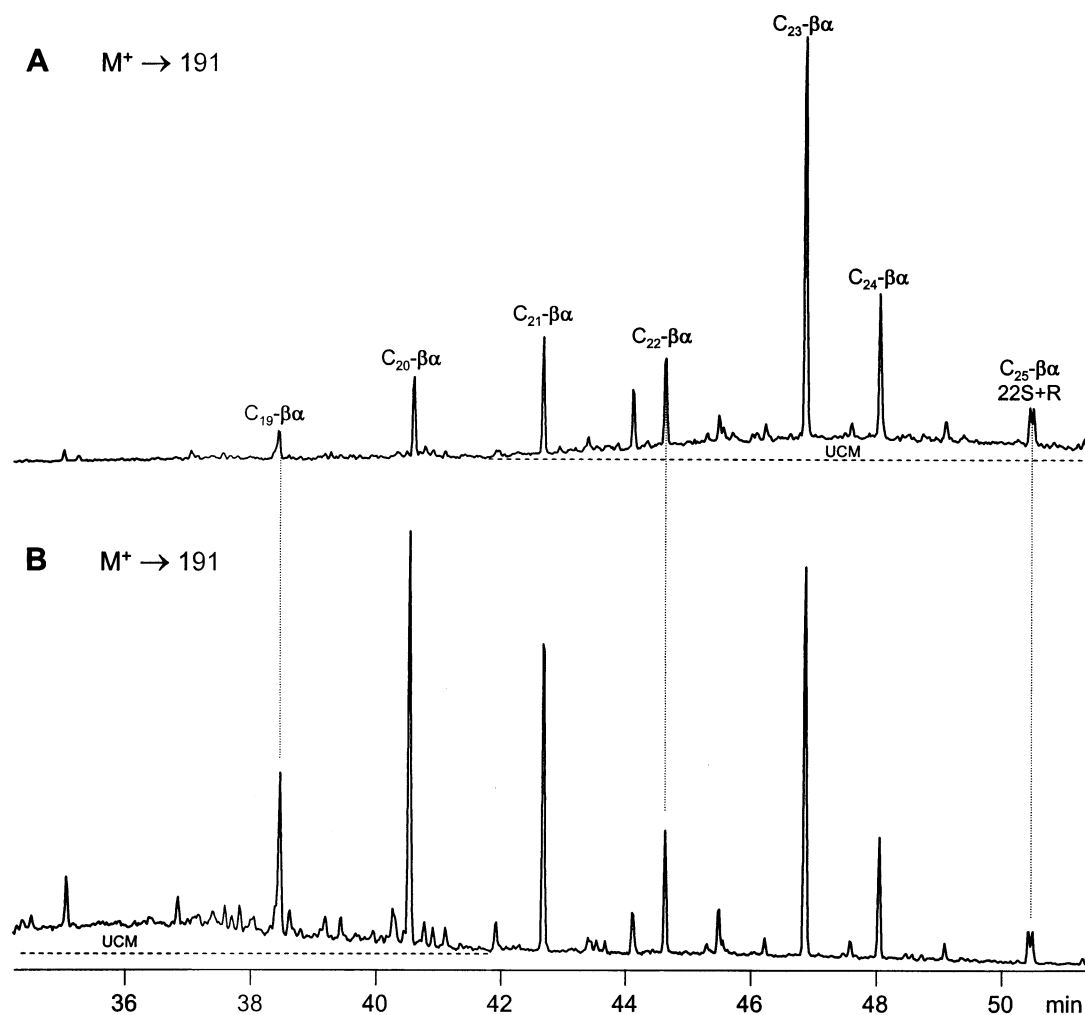
Fig. 5. Reconstructed GC-MS MRM-chromatograms of $M^+ \rightarrow 191$ transitions of C_{19} to C_{25}-13β(H),14α(H)-cheilanthanes (tricyclic terpanes). (A) *War5* from drill core WRL-1, representative of samples from the Fortescue Group. (B) *Bee1* from Mt Tom Price, representative of the Hamersley Group. UCM = Unresolved complex mixture.

function of physical redistribution processes or thermal degradation but not of biologic source. Therefore, abiological processes responsible for the shift of the UCMs may also have caused the differences in cheilanthane distribution.

3.2.4. Tetracyclic Diterpanes

GC-MS metastable reaction monitoring of the parent-daughter transition $274 \rightarrow 123$ revealed in some samples the presence of signals eluting in the same range as isomers of beyerane, phyllocladane and kaurane, biomarkers for higher plants. However, these MRM transitions were always close to the detection limit and so the identity and origin of the signals remains unresolved.

3.2.5. Hopanes

GC-MS metastable reaction monitoring (MRM) of pentacyclic terpanes revealed the presence of regular and rearranged hopanes in all samples in the ppb range (Table 1). It was

possible to detect the complete C_{27} to C_{35}-17α(H),21β(H)-hopane series in MRM $M^+ \rightarrow 191$ mass chromatograms (Fig. 6). C_{27}-hopanes are represented by 17α(H)-22,29,30-trinorhopane (Tm) and the diagenetic rearrangement product 18α(H)-22,29,30-trinorneohopane (Ts). The C_{28}-hopane 17α(H),21β(H)-29,30-dinorhopane (29,30-DNH) is probably a degradation product of 30-norbacteriohopanepolyols of unknown biologic origin. In the Pilbara bitumens it occurs in low relative concentrations, as in most bitumens and petroleums (Peters and Moldowan, 1993). 28,30-Dinorhopane (28,30-DNH) also occurs in the Pilbara rock extracts in trace amounts. 28,30-DNH is a common constituent of many bitumens and crude oils typically occuring in low concentrations (Mello et al., 1989). However, biologic sources or diagenetic precursors for 28,30-DNH are unknown although elevated concentrations are typical for highly reducing depositional environments (Mello et al., 1989). The regular C_{29}-hopane 17α(H),21β(H)-30-norhopane (C_{29}-$\alpha\beta$) is the most abundant pentacyclic terpane in all samples. The diagenetic rearrange-
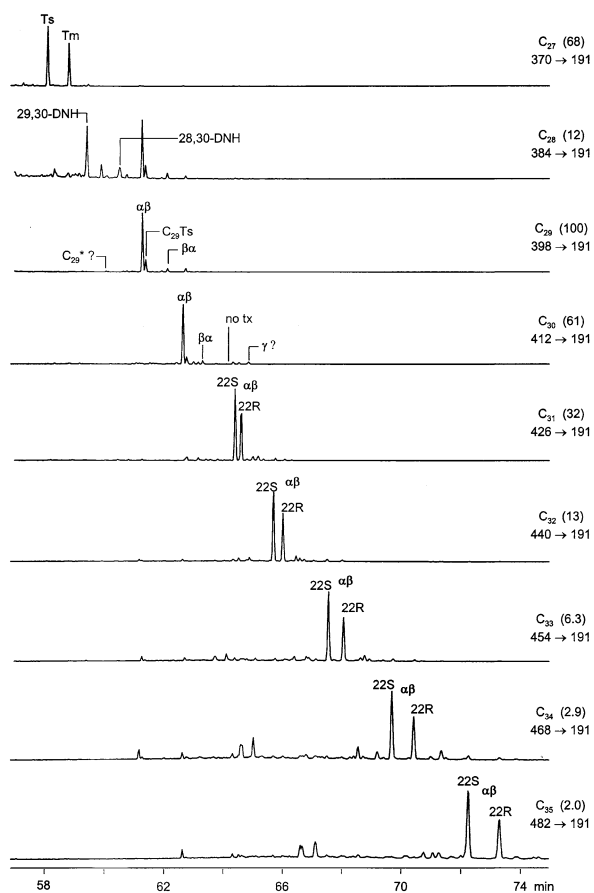
Fig. 6. Distribution of hopanes and other pentacyclic terpanes in the saturated fraction of sample *Mam1* from drill core WRL-1, Marra Mamba Iron Formation, Hamersley Group. Data was obtained by GC-MS MRM transitions $M^+ \rightarrow 191$. Chromatograms are identified by carbon number, the relative height (abundance) of the most intense peak in the trace, and the MRM reaction transition. tx = taraxastane, γ = gammacerane, $C_{29}{}^*$ = $17\alpha(H)$-diahopane. Other compound abbreviations are defined in the text.
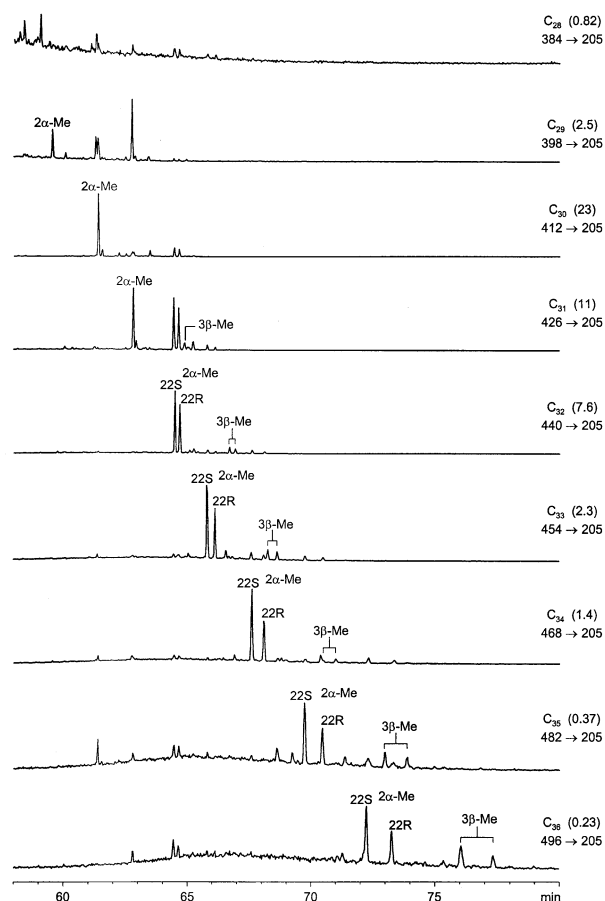
Fig. 7. Distribution of A-ring methylated hopanes in the rock extract of sample *Mam1* from drill core WRL-1, Marra Mamba Iron Formation, Hamersley Group. Data was obtained by GC-MS MRM transitions $M^+ \rightarrow 205$. Chromatograms are identified by carbon number, the relative height (abundance) of the most intense peak in the trace (continued from Fig. 6) and the MRM reaction transition. Compound abbreviations are defined in the text.

ment product $18\alpha(H),21\beta(H)$-30-norneohopane (C_{29}Ts; Moldowan et al., 1991) elutes just after C_{29}-$\alpha\beta$ in 398 $\rightarrow$ 191 chromatograms and was detected in concentrations 4 to 8 times lower than the C_{29}-$\alpha\beta$ isomer (Fig. 6; Appendix B, Table A2). $17\alpha(H),21\beta(H)$-Hopane (C_{30}-$\alpha\beta$) and extended $\alpha\beta$-hopanes with 31 to 35 carbon atoms are present in most of the Pilbara samples and rapidly decrease in concentration with increasing molecular weight (Fig. 6). Minor components eluting after each signal of the $17\alpha(H),21\beta(H)$-hopane series were identified as $17\beta(H),21\alpha(H)$-hopanes ($\beta\alpha$-hopanes or moretanes). The ratio of $\beta\alpha$-hopanes to $\alpha\beta$-hopanes is ~0.05 in all samples, a value described as the thermal equilibrium reached during early stages of oil generation (Peters and Moldowan, 1993). Trace compounds eluting shortly before regular $\alpha\beta$-hopanes in C_{29} to C_{34} MRM-chromatograms were tentatively identified as the $17\alpha(H)$-diahopane series first described by Moldowan et al. (1991) ($C_{29}{}^*$ in Fig. 6).

MRM $M^+ \rightarrow 205$ chromatograms of the Pilbara bitumens also indicate the presence of relatively high concentrations of A-ring methylated hopanes (Fig. 7). By plotting molecular

carbon number against the logarithm of retention times of individual signals, it was possible to identify the complete C_{29} to C_{36} 2α- and 3β-methylhopane series (filled symbols in Fig. 8; cf. Summons and Jahnke, 1992; note that the carbon numbers in the reference were not correctly plotted). Compounds eluting only a few seconds after each regular $\alpha\beta$-hopane with one carbon atom less were identified as C_{29} to C_{36}-2α-methyl-$17\alpha(H),21\beta(H)$-hopanes. The second series eluting shortly after the corresponding desmethyl $\alpha\beta$-hopanes with the same molecular weight are C_{31} to C_{36}-3β-methyl-$17\alpha(H),21\beta(H)$-hopanes.

3.2.6. Gammacerane, Taraxastane, Oleanane and Bicadinane

The MRM 412 $\rightarrow$ 191 transition in all bitumens shows a signal at the correct elution position for gammacerane (γ) (Fig. 6). However, concentrations were too low for an unambiguous identification. Taraxastane (tx) is a rearrangement product of lupanes and believed to be an indicator of terrestrial organic
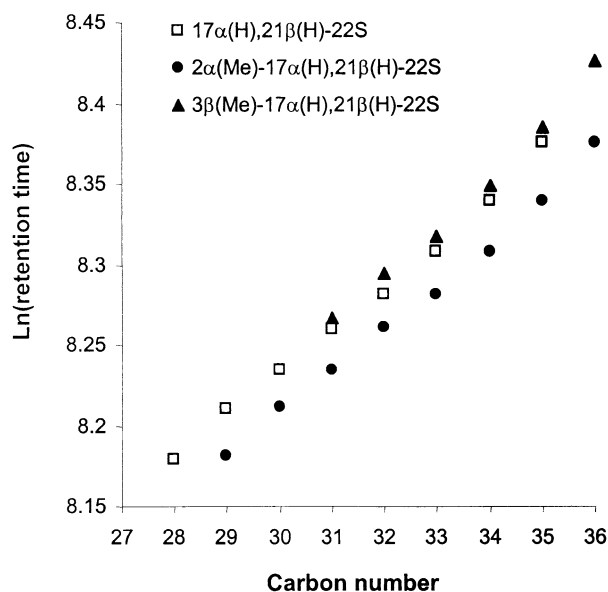
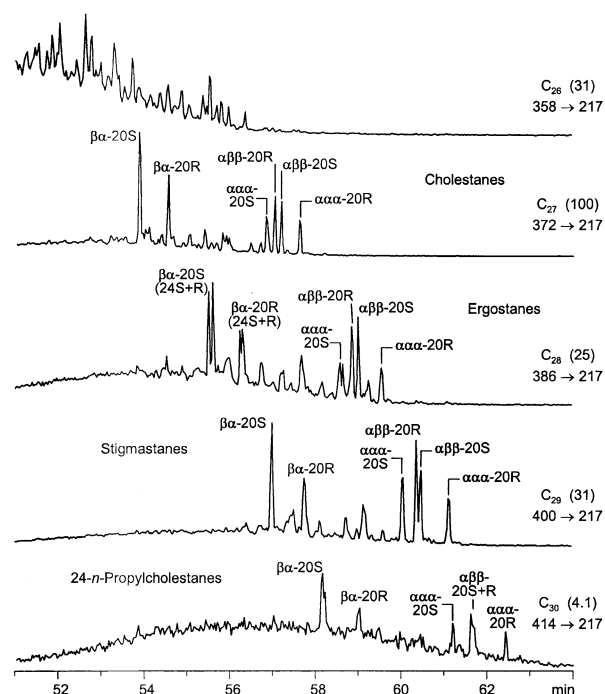Fig. 8. Correlation between the logarithm of retention times and carbon number for three hopane series.

Fig. 9. Distribution of steranes in sample *Roy3* from drill core WRL-1, Jeerinah Formation, Fortescue Group. Data was obtained measuring MRM transitions $M^+ \rightarrow 217$. Chromatograms are identified by carbon number, the relative height (abundance) of the most intense peak in the trace, and the MRM reaction transition. $\beta\alpha$ = $13\beta(H),17\alpha(H)$-diasteranes; $\alpha\alpha\alpha$ = $5\alpha(H),14\alpha(H),17\alpha(H)$-steranes; $\alpha\beta\beta$ = $5\alpha(H),14\beta(H),17\beta(H)$-steranes.

matter (Perkins et al., 1995). A low response close to the detection limit at the elution position of taraxastane in the 412 → 191 transition was not only visible in some samples from drill core WRL-1, but also in kerogen-poor control sample *Wal1*. Hence, the identity and origin of the recorded signals is uncertain. Oleanane, a diagnostic marker for higher plants, was absent from MRM 412 → 191 and 412 → 369 transitions (Peters and Moldowan, 1993) in all samples. Bicadinane, a fragmentation product of angiosperm dammar resin (van Aarssen et al., 1990; Anderson and Muntean, 2000) and frequently detected in Tertiary oils and bitumens, was present in extremely low concentrations in four samples (*FVG1*, *Dal1*, *Tum1*, and *Roy11*). However, similar quantities were also identified in a procedural blank and were probably introduced by cross contamination from younger samples processed in the laboratory.

3.2.7. Steranes and aromatic steroids

Steranes and aromatic steroid hydrocarbons also occur in the Pilbara bitumens. They comprise most of the known C_{26} to C_{30}-pseudohomologues, diasteranes (Fig. 9), A-ring methylated steranes (Fig. 10) and mono- and triaromatic steroids that have been recorded in the Proterozoic and Phanerozoic. Cholestane (C_{27}) was consistently the most abundant pseudohomologue comprising 42 to 58% of the total C_{27} to C_{29}-regularsteranes (Appendix B, Table A2), followed by stigmastane (C_{29}) comprising 26 to 36% and ergostane (C_{28}) comprising ~20%. 24-*n*-Propylcholestanes (C_{30}) comprise 2 to 4% of total C_{27} to C_{30}-regular steranes. 24-Isopropylcholestane, a biomarker for sponges and particularly abundant in Cambrian and Neoproterozoic carbonates (McCaffrey et al., 1994), was not observed in the Pilbara samples.

Diasteranes form by diagenetic rearrangement of functionalized steroid precursors (Sieskind et al., 1979). They generally increase in abundance relative to regular steranes (Dia/Reg)

with increasing clay content and decreasing kerogen content of the source rock (van Kaam-Peters, 1997). Dia/Reg might also increase with thermal maturity (Goodarzi et al., 1989) and might be influenced by chromatographic processes during subsurface fluid flow (Zhusheng et al., 1988). In the Pilbara bitumens, the relative concentration of diasteranes to regular steranes is subject to large variations (Appendix B, Table A2). Dia/Reg ratios in core WRL-1 fluctuate between 0.56 and 1.3. The lowest values in WRL-1 occur in the upper section of the core that comprises the lowermost Hamersley Group (Dia/Reg = 0.56 to 0.70 in *Mam1*, *Mam2* and *Mam3*; Appendix B, Table A2) and increase in the underlying Fortescue Group (Dia/Reg = 0.70–1.3). Dia/Reg ratios in the Hamersley Group from Mt Tom Price and Mt Whaleback are also on average lower than in samples from the Fortescue Group, ranging from 0.36 to 0.80. The observed values are generally consistent with the clay-rich nature of the Archean host rocks and with high thermal maturities.

As for the regular steranes, the most abundant diasteranes in all Pilbara samples are the C_{27}-isomers (Appendix B, Table A2). However, diasteranes do not have the same strict $C_{27} > C_{29} > C_{28}$ abundance order as the regular steranes. C_{28}-pseudohomologues are either equally abundant as C_{29} (WRL-1 samples), more abundant than C_{29} (Hamersley Group at Mt Tom Price) or less abundant than C_{29} diasteranes (Hamersley Group at Mt Whaleback).

Steranes methylated at ring-A also occur in all samples. MRM measurements of the C_{30} 414 → 231 transition reveal the
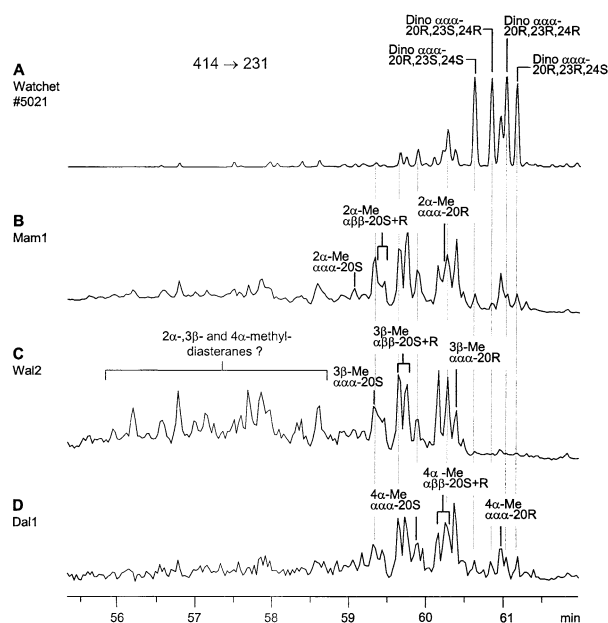
Fig. 10. Distribution of C_{30} A-ring methylated steranes measured by GC-MS MRM transition $414 \rightarrow 231$. (A) A Triassic bitumen (Watchet #5021) with high relative concentrations of dinosteranes, (B) sample *Mam1* from drill core WRL-1, Marra Mamba Iron Formation, Hamersley Group, (C) sample *Wal2* from Mt Whaleback, Brockman Iron Formation, Hamersley Group, (D) sample *Dal1* from Mt Tom Price, Brockman Iron Formation, Hamersley Group. Dino $\alpha\alpha\alpha = 4\alpha$-methyl-$5\alpha(H),14\alpha(H),17\alpha(H)$-23,24-dimethylcholestane.
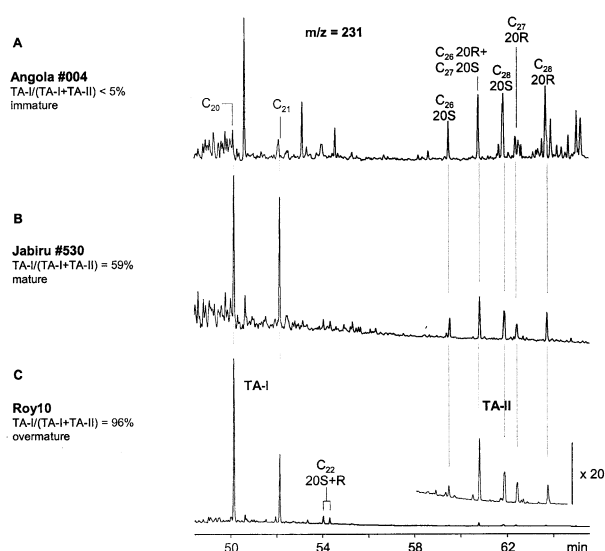

Fig. 11. Distribution of triaromatic steroids in GC-MS $m/z = 231$ selected ion chromatograms detected in (A) an immature Phanerozoic oil (Angola AGSO#004), (B) a mature Phanerozoic oil (Jabiru AGSO#530) and (C) sample *Roy10* from drill core WRL-1, Jeerinah Formation, Fortescue Group. The inset in (C) is a 20× magnification of the elution range of C_{26}- to C_{28}-triaromatic steroids. Signals identified according to Peters and Moldowan (1993).

presence of 2α-, 3β- and 4α-methy-24-ethylcholestanes including $\alpha\alpha\alpha$-20S and R, and $\alpha\beta\beta$-20S and R isomers (Fig. 10). These C_{30}-methylsteranes are 1.5 to 5 times lower in abundance than the corresponding non-methylated C_{29} steranes. Dinosteranes (4α,23,24-trimethylcholestanes) were also detected in MRM $414 \rightarrow 231$ transitions of some samples, although concentrations were generally low. The weak signals were assigned by comparison to retention times of a Triassic bitumen known to contain very high concentrations of dinosteranes (Fig. 10A; cf. Fig. 2 in Summons et al., 1992; see also Summons et al., 1987). The $386 \rightarrow 231$ and $400 \rightarrow 231$ transitions similarly show several isomers of C_{28} and C_{29} A-ring methylated steranes. Steranes with a C_2-substitution pattern upon ring-A are also present in low relative concentrations.

C-ring monoaromatic steroids (MA) were detected by SIR of the most intense fragment ion $m/z = 253$. In most samples C_{27} to C_{29}-MA were below the detection limit and only the thermally degraded C_{21} to C_{22}-pseudohomologues were identified. The low concentration of all monoaromatic steroids was probably caused by maturity-driven aromatization to triaromatic steroids (TA) (Mackenzie et al., 1981). The high degree of aromatization from monoaromatic to triaromatic steroids in the Pilbara bitumens is indicated by TA/(TA + MA) > 90% (Appendix B, Table A3). Like the monoaromatic steroids, triaromatic steroids, identified in SIR $m/z = 231$ chromatograms, were strongly affected by thermal degradation of the D-ring side chain. Therefore, triaromatic steroids with 26 to 28 carbon atoms are only present in trace amounts while the

thermal degradation products C_{20} and C_{21}-TA are very abundant (Fig. 11C). Triaromatic steroids of the $m/z = 245$ series with an extra methyl-group on rings A to C were also observed.

3.2.8. Aromatic hydrocarbons

The Pilbara rock extracts contain mostly mono- to tricyclic aromatic hydrocarbons, with polyaromatic hydrocarbons (PAH) with four or more rings occurring only in very low concentrations. However, the distribution of mono- to tricyclics falls into two distinctive groupings. The first grouping includes all samples from the Fortescue Group and the Marra Mamba Iron Formation (lowermost Hamersley Group) (Figs. 12A and 12B). In these samples the concentration of parent PAH is low relative to their methylated homologues (MePAH) (Appendix B, Table A3; Fig. 12). Similar aromatic hydrocarbon distributions are common in most Proterozoic and Phanerozoic bitumens and oils. The second grouping includes all samples (except *Rae2*) from the Hamersley Group near Mt Tom Price and at Mt Whaleback. Parent PAH are more abundant than methylated homologues, and aromatic compounds with two or more substituents occur in very low relative concentrations (Fig. 12D). Thus, PAH/MePAH ratios are predominantly > 1, even exceeding 100 in some samples (Appendix B, Table A3).

3.3. Carbon Isotopic Composition of Individual Hydrocarbons and Kerogen

Appendix B, Table A4 contains the carbon isotopic composition of the kerogen and individual hydrocarbons for a suite of Pilbara samples. Kerogens from mudstones of the Mt McRae Shale and the Brockman Iron Formation, both Hamersley Group, fall into the $\delta^{13}C$ range of -32 to $-35‰$. Kerogens of
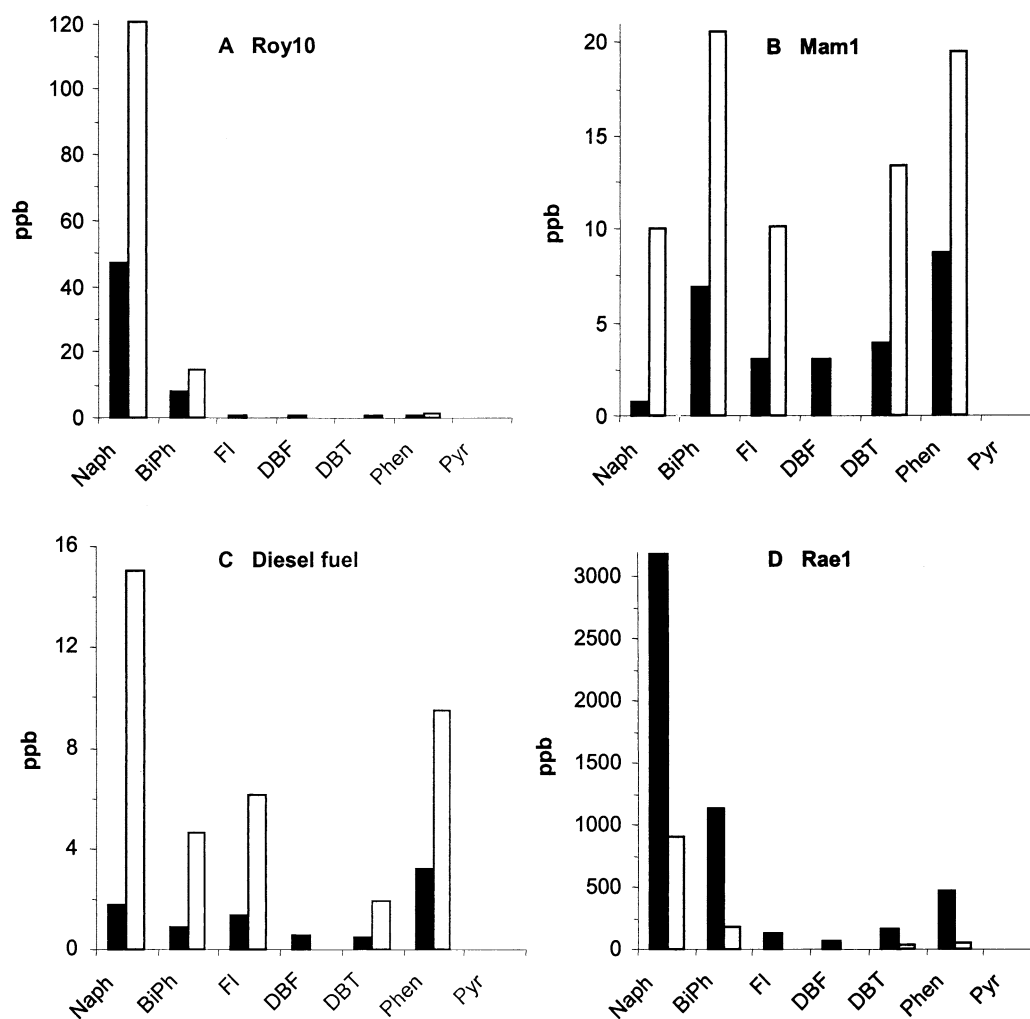
Fig. 12. Absolute concentrations of parent and monomethylated aromatic hydrocarbons and dibenzothiophene. Naph = naphthalenes; BiPh = biphenyls; Fl = fluorenes; DBF = dibenzofurans; DBT = dibenzothiophenes; Phen = phenanthrenes; Pyr = pyrenes. Black bars = unsubstituted parent compounds; white bars = the sum of all isomers of the corresponding monomethylated homologues. The y-axis indicates absolute concentrations in parts per billion (nanograms per gram of extracted rock). (A) Sample *Roy10* from drill core WRL-1, Jeerinah Formation, Fortescue Group. (B) Sample *Mam1* from drill core WRL-1, Marra Mamba Iron Formation, Hamersley Group. (C) Diesel fuel. (D) Sample *Rae1* from drill core G1185-81 from Mt Tom Price, Mt McRae Shale, Hamersley Group.

the upper Fortescue Group to lowermost Hamersley Group are isotopically light with $\delta^{13}C$ of -37 to $-47‰$. These $\delta^{13}C_{kerogen}$ values are typical for rocks of the Fortescue and Hamersley Group (Hayes et al., 1983).

In bitumens from the Mt McRae Shale and Brockman Iron Formation n-alkanes are isotopically enriched in ^{13}C relative to kerogen by 2 to 6‰, and in the upper Fortescue to lowermost Hamersley Group they are enriched by 11 to 21‰. The acyclic isoprenoids pristane and phytane are depleted in ^{13}C up to 3‰ relative to the n-alkanes. In a limited number of Mt Tom Price bitumens it was possible to determine $\delta^{13}C$ of individual aromatic hydrocarbons (Appendix B, Table A4). The carbon isotopic composition of unsubstituted PAH in Mt McRae shale samples *Rae1* and *Bee1* is -30 to $-34‰$, which is similar to the $\delta^{13}C_{kerogen}$ of -32.2 and $-33.5‰$, respectively. Concentrations of polycyclic biomarkers were too low for isotopic ratio measurements.

3.4. Bitumen Thermal Maturity

3.4.1. n-Alkane distribution

The n-alkane profile in most Pilbara extracts has a condensate-like distribution, such that low molecular weight n-alkanes are very abundant and the concentration of higher homologues decreases rapidly with increasing carbon number (Fig. 3). These distributions are very similar to a South Texas gas-condensate that exists at a present day temperature of $\sim200°C$ and has been reservoired at this temperature for ~30 Ma (McNeil and BeMent, 1996). Condensate-like compositions can result from thermal cracking and/or fractionative distillation associated with condensation of hydrocarbons from a gas phase (Thompson, 1987, 1988). The n-alkane profiles of the Pilbara samples therefore indicate a maturity in the wet-gas zone and are consistent with temperatures of $\sim200°C$.

Table 3. The relationship between the methyladamantane index (MAI), the methyldiamantane index (MDI) and vitrinite reflectance (R_o) determined for samples from two Chinese basins.[a]

MAI[b] (%)	MDI[c] (%)	R_o (%)
50–70	30–40	1.1–1.3
70–80	40–50	1.3–1.6
80–90	50–60	1.6–1.9
>90	>60	>1.9

[a] Adopted from Table 3 in Chen et al. (1996).
[b] MAI = 1-MA/(1-MA + 2-MA). MA = methyladamantane.
[c] MDI = 4-MD/(1-MD + 3-MD + 4-MD). MD = methyldiamantane.

3.4.2. Methyladamantane and Methyldiamantane indices

Chen et al. (1996) introduced the methyladamantane index (MAI) and the methyldiamantane index (MDI) as indicators of overmature crude oils and condensates. The authors found good linear correlations between MAI, MDI and vitrinite reflectance (R_o) in the range R_o = ~ 1.1 to ~ 1.9% (Table 3). However, at higher maturities methyladamantane and methyldiamantane indices are poorly defined and inverted trends are possible. For example, at R_o > 1.9% MDI values were shown to fluctuate between 38 and 65% (Jinggui et al., 2000).

The methyladamantane and methyldiamantane indices obtained from the Pilbara samples generally indicate high thermal maturities. The diamondoid hydrocarbons are particularly abundant in bitumens from the Hamersley Group at Mt Tom Price and Mt Whaleback and MAI ranges from 70 to 97% (Appendix B, Appendix B, Table A3). By comparison with the Chen scale in Table 3, these values translate into reflectance equivalents R > 1.3% to R ≫ 2% (Table 3), corresponding to thermal maturities in the wet-gas and possibly even the dry-gas zone. The high MDI values in the Pilbara samples of 60% are consistent with wet-gas zone or higher maturity. In the Fortescue and lower Hamersley Group signal-to-noise ratios of the diamondoid mass spectrometry signals were comparatively low and, therefore, reliable values for MAI and MDI only available for a limited number of samples (Appendix B, Table A3). However, the measured values correspond to vitrinite reflectances R = 1.2 to > 1.9%, consistent with the late stage of oil generation to the wet-gas zone.

3.4.2.1. The unusual composition of Mt McRae shale sample Rae6.

Bitumen *Rae6* extracted from the Mt McRae Shale at Mt Tom Price has a unique hydrocarbon assemblage. It consists exclusively of diamondoids, parent PAH and minor concentrations of alkylated PAH. Aliphatic hydrocarbons were not detected. Similarly, high proportions of diamondoids have also been reported from condensates produced in deep subsurface dry-gas reservoirs in the Gulf of Mexico (Dahl et al., 1999). Generally, the thermally highly stable adamantanes and diamantanes become concentrated in oil and gas by the preferential degradation of all other molecular components (Dahl et al., 1999). Therefore, the preservation of high relative concentrations of diamondoids in *Rae6*, the absence of other saturated hydrocarbons, and the high relative concentrations of parent PAH suggest a thermal maturity in the dry-gas zone for this particular sample.

3.4.3. Sterane and Hopane isomer ratios

Sterane and hopane ratios conventionally used to assess thermal maturity apparently reach their end-values within the oil-generation window and therefore cannot be used to evaluate overmature bitumens and gas-condensates. However, they can be used to assess possible contamination from less mature organic matter. For example, in all Pilbara samples the epimer ratio 22S/(22S + 22R) for extended $\alpha\beta$-hopanes is at the thermodynamic end point value of ~ 0.5 (Appendix B, Table A2; cf. Peters and Moldowan, 1993). The C_{27} to C_{29}-sterane isomer ratios 20S/(20S + 20R) and $\alpha\beta\beta/(\alpha\beta\beta + \alpha\alpha\alpha)$ have reported thermal equilibrium values of ~0.55 and ~0.70 respectively, values apparently reached close to the peak of oil generation (Peters and Moldowan, 1993). In the Pilbara solvent extracts the sterane ratios show large variations, even between samples collected from the same drill core (20S/[20S + 20R] = 0.6 ± 0.2; $\alpha\beta\beta/[\beta\beta\beta + \alpha\alpha\alpha]$ = 0.55 ± 0.1; Appendix B, Table A2). The isomer ratios are below the recorded maximum values in some samples and above in others. However, similar fluctuations have been detected in overmature bitumens close to igneous intrusions (Raymond and Murchison, 1992). Moreover, inversion of 20S/(20S + 20R) and $\alpha\beta\beta/(\alpha\beta\beta + \alpha\alpha\alpha)$ to lower values was observed in pyrolysis experiments at temperatures above 300°C (Peters et al., 1990). The sterane and hopane maturity parameters are therefore consistent with, albeit not indicative of, maturities above the oil generation window.

3.4.4. Mono- and Triaromatic steroid maturity parameters

Parameters based on mono- and triaromatic steroids can be used to assess thermal maturity above the oil generation window (Mackenzie et al., 1981). With increasing thermal maturity C-ring monoaromatic steroids (MA) undergo aromatization to triaromatic steroids (TA) and the degree of aromatization is measured by the ratio TA/(TA + MA). Most Pilbara bitumens have TA/(TA + MA) > 90% (Appendix B, Table A3), consistent with maturities in the wet-gas zone (Mackenzie et al., 1981; Peters et al., 1990).

Thermal cracking of the side chain of C_{26} to C_{28}-triaromatic steroids (TA-II) leads to the generation of degradation products with 20 to 21 carbon atoms (TA-I), and TA-I/(TA-I + TA-II) is apparently sensitive for thermal maturities above the oil-generation window (Riolo et al., 1985). The distributions of triaromatic steroids in the transition from immature through mature to overmature petroleum is illustrated in Figure 11. In most Pilbara bitumens the destruction of C_{26} to C_{28}-triaromatic steroids is close to complete (Fig. 11C) and TA-I/(TA-I + TA-II) is > 90% (Appendix B, Table A3). Values in this range, according to Peters and Moldowan (1993), indicate thermal maturities in the wet-gas zone. The low triaromatic steroid parameters for samples from drill core FVG-1 (50–60%) possibly indicate bitumen within the oil window which seems inconsistent with the thermal history of the host rock.

3.4.5. Aromatic maturity parameters

Ratios of aromatic hydrocarbons and dibenzothiophenes are frequently used to assess petroleum maturity (Radke et al., 1982a). However, the application of maturity parameters based on naphthalenes, phenanthrenes and dibenzothiophenes to bitumens of Archean age is problematic because the aromatic compounds used to calculate these ratios are also strongly source dependent and require different calibrations for various organic matter (Radke et al., 1986). However, calibration is not available for Paleoproterozoic to Archean kerogens (Boreham et al., 1988). Moreover, the behavior of aromatic isomer ratios in overmature source rocks is poorly understood. At very high maturities, some ratios have been shown to reverse trends (Radke et al., 1982b) or become unpredictable (Raymond and Murchison, 1992). Hence, the ability of aromatic hydrocarbons to assess the thermal maturity of bitumens extracted from different Archean metasedimentary rocks is limited. However, in some specific instances, the methylphenanthrene index (MPI-1), the methylphenanthrene ratio (MPR), the methylphenanthrene distribution factor (MPDF), the methyldibenzothiophene ratio (MDR) and ratios of unsubstituted to monomethylated aromatic compounds (PAH/MePAH) might be useful for indicating overmature or pyrolyzed bitumen.

MPI-1 ($1.5 \times$ [2-MP + 3-MP]/[Phen + 1-MP + 9-MP]) apparently reaches its maximum value at a vitrinite reflectance equivalent of $R \approx 1.7\%$ and then decreases with higher maturities (Boreham et al., 1988; Radke et al., 1982a). This trend "reversal" is related to demethylation of methylphenanthrenes to phenanthrene. So low MPI-1 values can be indicative of immature or highly mature bitumen, but a reversed MPI-1 can be recognized by high phenanthrene/methylphenanthrene ratios (Phen/MP > 1) (Appendix B, Table A3). A second factor influencing MPI-1 and MPDF ([3-MP + 2-MP]/[3-MP + 2-MP + 9-MP + 1-MP]) is the kinetically controlled methylation of phenanthrene. At low temperatures phenanthrene reacts with methyl donors to yield predominantly 9-methylphenanthrene (Alexander et al., 1995). Bitumen with high relative concentrations of phenanthrene might therefore also contain high relative concentrations of 9-methylphenanthrene resulting in 9-MP/1-MP ratios > 1 and lower MPI-1 and MPDF values (Appendix B, Table A3). Less affected by demethylation and methylation reactions than MPI-1 and MPDF is MPR (2-MP/1-MP). Therefore, MPR might be the most reliable phenanthrene parameter for overmature bitumen (Appendix B, Table A3). The PAH/MePAH ratio is not usually applied as a maturity parameters but is potentially indicative of extreme maturities and pyrolytic conditions. Thermal decomposition of alkylated aromatics leads to progressive loss of side chains and an increase in the concentration of the parent compounds (Radke et al., 1982a; Price, 1993).

Phenanthrene maturity parameters in samples from drill cores WRL-1 and FVG-1 (Fortescue Group to lowest Hamersley Group) indicate maturities within the oil generation window based on standards for younger source rocks (Radke et al., 1986; Boreham et al., 1988). Eqn. 3 and 5 in Boreham et al. (1988) can be used to estimate vitrinite reflectance equivalents (R_c) from MPDF and MPI-1. If applied to the Pilbara bitumens from WRL-1 and FVG-1, $R_c \approx 0.7$ to 1.1%. These values are roughly equivalent to early to late stages of oil generation.

Table 4. Aromatic maturity parameters and vitrinite reflectance for sample *Tum1* from the Tumbiana Formation, Fortescue Group, and sample E15, a contact metamorphosed shale from the Jurassic Posidonien Schiefer in Northwest Germany.

	Phen/MP[a]	MPI-1[b]	MPR[c]	R_c (%)[d]	R_m (%)[e]
E15[f]	0.8	0.76	1.5	2.6	2.5
Tum1	1.5	0.46	1.9	2.7	—

[a] Compound abbreviations are defined in Appendix B, Table A3. Phen/MP = Phen / (1-MP + 2-MP + 3-MP + 9-MP).
[b] MPI-1 = $1.5 \times$ (2-MP + 3-MP) / (Phen + 1-MP + 9-MP).
[c] MPR = 2-MP/1-MP.
[d] Calculated vitrinite reflectance equivalent R_c (%) = $-0.55 \times$ (MPI-1) + 3.0 (Eqn. 5 in Boreham et al., 1988).
[e] R_m = measured vitrinite reflectance.
[f] Radke et al. (1986).

The sample *Tum1* from drill core SV-1, lower Fortescue Group, shows substantially higher phenanthrene related maturity compared to samples from WRL-1 and FVG-1. The high Phen/MePhen ratio of 1.5 indicates that the low MPI-1 value of 0.46 is due to dealkylation of methylphenanthrenes at very high thermal maturity equivalent to $R_c = 2.7\%$ (Eqn. 5 in Boreham et al., 1988). This result is also supported by a high MPR (1.9) and MPDF (0.61) (Appendix B, Table A3). The phenanthrene maturity parameters of sample *Tum1* are also similar to a sample from the Jurassic Posidonien Schiefer in northwest Germany that was metamorphosed by an igneous intrusion and has a measured vitrinite reflectance of $R_m = 2.5\%$ (sample Eqn. 15 in Radke et al., 1986; Table 4).

The aromatic hydrocarbon fractions from the Hamersley Group at Mt Tom Price and Mt Whaleback show characteristics of pyrolytic alteration. In all samples, except one, most PAH/MePAH ratios are $\gg 1$ (Appendix B, Table A3), indicating maturities in the wet-gas zone or higher. Consistent with this interpretation are the very low, inverted MPI-1 values of 0.14 to 0.06 that are equivalent to $R_c > 3\%$ (Boreham et al., 1988). High relative concentrations of parent versus alkylated PAH have been previously observed in modern and fossil hydrothermal environments (Simoneit, 1993), in proximity to igneous intrusions (George, 1992) and in association with copper mineralization (Püttmann et al., 1988). Shales collected at Mt Tom Price and Mt Whaleback are closely associated with large deposits of secondarily enriched iron ore. This suggests the mechanisms of iron remobilization and the generation of high concentrations of unsubstituted PAH are probably related.

3.5. Arguments for and Against Syngeneity

3.5.1. Laboratory procedural blanks

Procedural blanks were run parallel to each set of five samples to monitor laboratory introduced contamination. Aromatic and saturated hydrocarbons in blanks were always below GC-FID detection limit. Scanning by highly sensitive GC-MS-MS, however, revealed traces of sterane and hopane biomarkers in the blanks. The influence of this background contamination was monitored by calculating the concentration of individual biomarkers in samples relative to their concentration in the blank (extract/blank ratio) (Appendix B, Table A5). For

example, an extract/blank ratio of 3100 for C_{27}-$\beta\alpha$-20S-diasterane in *Roy1* indicates that this particular compound is 3100 times more abundant in the rock extract than in the procedural blank. Biomarker parameters in samples where one or more compounds have an extract/blank ratio < 20 were not used in the present study to characterize samples and are printed in italics in Appendix B, Table A2. The concentration of sterane and hopane biomarkers was high in most mudstones from the Fortescue and Hamersley Groups (extract/blank ratio ≫ 20) but negligible in samples with low kerogen contents (Appendix B, Table A5). In kerogenous samples *Rae3*, *Rae4*, *Rae6*, *War2* and *Tum1*, the extract/blank ratios were also < 20 and so their biomarker data was consequently interpreted as potentially non-indigenous. In all other samples, however, the procedural blanks have established that biomarkers and other hydrocarbons are not laboratory artifacts but components of the sampled rock.

3.5.2. Comparison of Kerogen-Rich and Kerogen-Poor rocks

The analysis of procedural blanks detects any contaminants that may have been introduced into rock extracts during laboratory procedures. To monitor contaminants that may have been introduced into rock samples before laboratory processing, for example during collection, transport or rock powder preparation, rocks devoid of kerogen (blank rocks) were analyzed along with the actual samples. Blank samples are volcanic or kerogen-poor sedimentary rocks collected at the same outcrop or from the same drill core as kerogen-rich source rocks. The results of blank rock analyses for drill core WRL-1 are graphically summarized in Figure 13. Extracts from blank rocks (left panel in Fig. 13) have far lower extract yields than kerogenous samples (right panel in Fig. 13) and also do not contain light alkanes < C_{16}. Results of bulk analyses, biomarker ratios and extract/blank ratios for some blank rock experiments are included in Table 1, and Appendix B, Tables A2 and A5, and identified by an asterisk (*). The absolute hopane and sterane concentrations per gram of extracted rock were one to two orders of magnitude lower in all blank rocks (except in kerogen-free mudrock *Mam3*) than in kerogenous host rocks (Table 1). The high hydrocarbon concentrations in kerogen-rich rocks, in contrast to blank rocks, strongly suggests that the samples were not contaminated during sampling, cutting, transport or rock powder preparation.

A previous study of drill core WRL-1 (Brocks et al., 1999) argued that the analysis of representative blank-rocks could also be used to detect migrated petroleum and drilling additives. However, oil that had migrated into the Archean rocks or entered the samples during drilling might have preferentially evaporated from kerogen-free rocks during their extended storage period (the core WRL-1 was drilled in 1986). Hydrocarbons absorbed by kerogen, on the other hand, would have been protected against evaporative loss (Oehler, 1977). Therefore, hydrocarbons detected in kerogen-free rocks may only reflect recent contamination events. However, bitumen-like hydrocarbons in blank rocks that were geologically closely associated with kerogen-rich samples should not automatically be attributed to contamination. For example, blank rocks *Mam3*, *Roy4* and *Roy6* from WRL-1 contain C_{17+} hydrocarbons with a distribution similar to adjacent highly kerogenous shales (Fig.

13). It is possible that these hydrocarbons are residues of petroleum that was expelled from adjacent source rocks.

3.5.3. Comparison of stable carbon isotopes of Kerogen and Bitumen

Rock extracts from the Hamersley Group are enriched in ^{13}C by 2 to 6‰ relative to co-occurring kerogens, and bitumens from the upper Fortescue to lowermost Hamersley Group by 11 to 21‰ (Appendix B, Table A4). This is in contrast to Phanerozoic bitumens and oils that are typically 2 to 4‰ lighter than the source kerogens (Hayes et al., 1983; Logan et al., 1997). Accordingly it has been argued that hydrocarbons extracted from Precambrian rocks that are > 2‰ heavier than co-occurring kerogen are very likely not indigenous (Hoering, 1965, 1966; Hayes et al., 1983). However, more recent work indicates that indigenous Proterozoic bitumen is indeed frequently ^{13}C enriched relative to kerogen (Logan et al., 1995, 1997). For example, the 600-Ma Pertatataka Formation contains C_{16}-C_{20} *n*-alkanes which are up to 6‰ heavier than the kerogen (Logan et al., 1999), and the terminal Proterozoic Huqf Formation contains $C_{23}+$ *n*-alkanes enriched by up to 8‰ compared to its kerogen (Höld et al., 1999). Although the isotopic disparity in many kerogen/bitumen pairs from the Fortescue Group is more extreme than in other Precambrian samples, this may represent an important characteristic of many Archean and Proterozoic ecosystems rather than a consequence of contamination. A hypothetical biologic model for the isotopic disparity is described in Brocks et al. (2003).

3.5.4. Comparison of Bitumen maturity and thermal history of the host rock

The composition of syngenetic bitumen must be consistent with the thermal history of its host rock. The samples of the Hamersley and Fortescue Groups have experienced regional metamorphism to prehnite-pumpellyite facies corresponding to temperatures between 200 to 300°C (Chapter 2). Therefore, any syngenetic bitumen that has been preserved should have a maturity in the wet-gas to dry-gas zone.

1. Bitumens from drill core WRL-1 (Fortescue Group and lowermost Hamersley Group) can be classified as gas-condensates based on their *n*-alkane distribution and mono- and triaromatic steroid maturity parameters. Sterane, hopane, methyladamantane and methyldiamantane maturity indices are all consistent with this interpretation. Maturity parameters based on aromatic hydrocarbons, on the other hand, suggest lower maturities, although the interpretation of these ratios in overmature Precambrian samples is certainly problematic. The compositions of the saturated hydrocarbon fractions are thus largely consistent with the metamorphic history of the host rock.

2. Rock extracts from drill core FVG-1 (Fortescue Group) have *n*-alkane distributions shifted to higher homologues in comparison to most other samples, as well as lower sterane and steroid maturity parameters. The compositions of extracts from FVG-1 correspond to a maturity within the oil generation window which is inconsistent with the metamorphic history of the host rock.

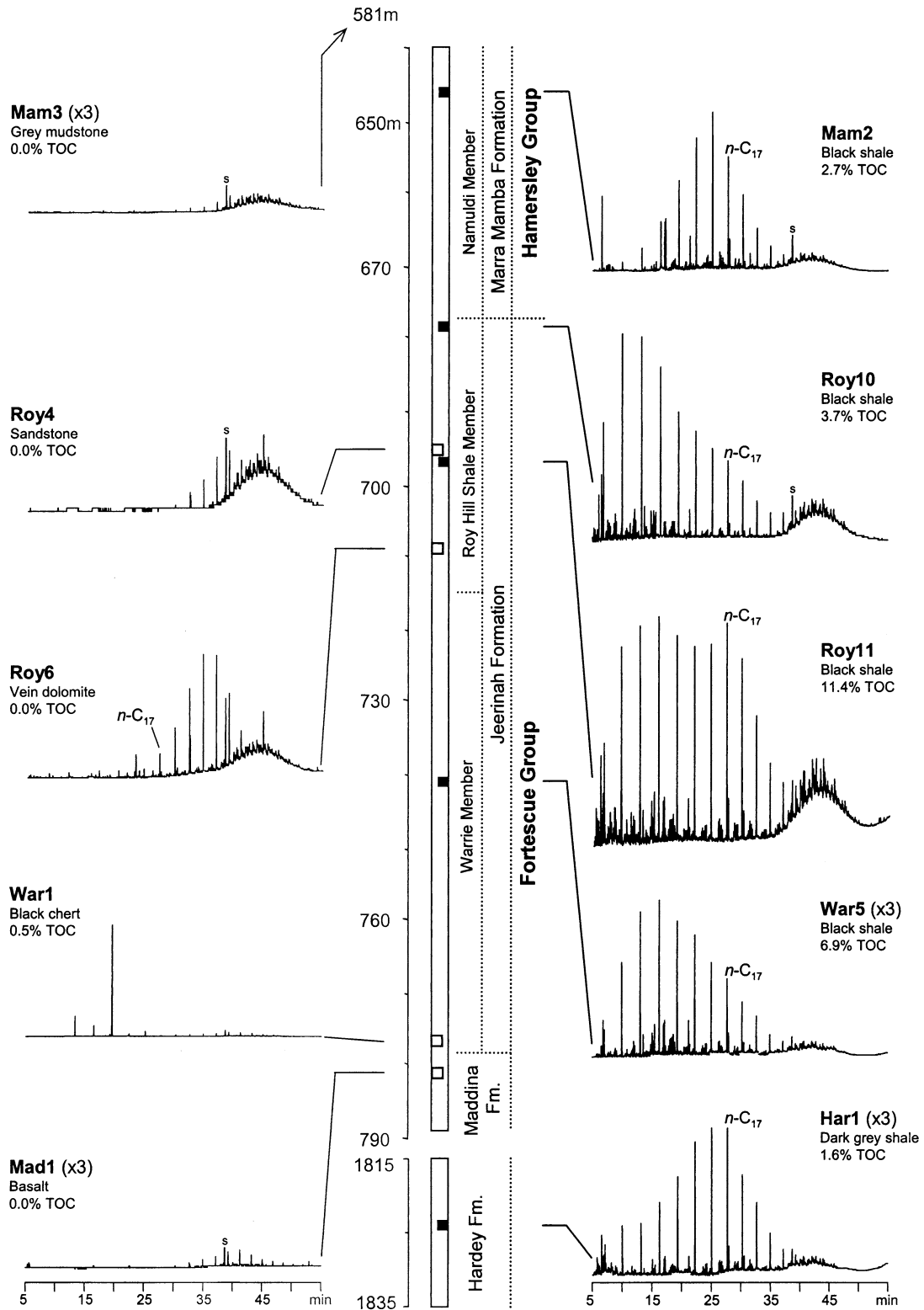Fig. 13. Drill core WRL-1 showing gas chromatograms of saturated hydrocarbons at different depths. Chromatograms are identified by sample name and kerogen content of the host rock. Kerogen-poor samples are shown on the left and kerogen-rich samples on the right. Signal heights are normalized to absolute extract concentrations per gram of rock ('×3' indicates magnification by factor 3 relative to unmagnified chromatograms).

3. Sample *Tum1* from drill core SV-1, lower Fortescue Group, was collected in one of the least metamorphosed areas on the craton. *n*-alkanes are slightly shifted to higher molecular weights in comparison to WRL-1 and are consistent with a condensate that has suffered evaporative loss of lighter components. Mono- and triaromatic steroid ratios and phenanthrene maturity parameters are consistent with a maturity in the wet-gas zone and appear consistent with the thermal history of the host rock.

4. Bitumens of the Hamersley Group from Mt Tom Price and Mt Whaleback have *n*-alkane distributions, mono- and triaromatic steroid parameters, methyladamantane and methyldiamantane ratios, PAH/MePAH ratios and phenanthrene maturity parameters indicative of maturities in the wet-gas zone. However, maturity values within the Tom Price area vary considerably. Mt McRae Shale sample *Rae2* from the B26 deposit, 24 km west of Mt Tom Price, has far lower PAH/MePAH ratios and phenanthrene maturity parameters than most other samples from this area, while *Rae6* consists entirely of polyaromatic hydrocarbons and diamondoids indicating dry-gas zone maturity. The thermal maturities of bitumens from Mt Tom Price and Mt Whaleback are probably consistent with the regional metamorphic grade but apparently also reflect local temperature differences possibly induced by hydrothermal activity or igneous intrusions.

The following list ranks the bitumens from different locations in the Hamersley Basin with increasing apparent maturity: drill core FVG-1 $<$ drill core WRL-1 $\sim$ drill core SV-1 $\sim$ sample *Rae2* (B26 deposit) $<$ Mt Tom Price $\leq$ Mt Whaleback $<$ sample *Rae6* (Mt Tom Price). This order is based on a very limited number of samples and is therefore tentative. However, apart from FVG-1, the order is consistent with regional models of metamorphism predicting that areas closer to the southern orogenic margin of the craton (Mt Tom Price, Mt Whaleback) should have higher maturities than samples from areas further north (SV-1 and WRL-1) (Fig. 1, Table 2). The considerable variation in thermal maturities of bitumens from the Mt Tom Price area is consistent with models that suggest ore formation was controlled by hydrothermal processes (Barley et al., 1999).

3.5.5. Age-Diagnostic patterns

The bitumens extracted from the Pilbara rocks have a molecular and isotopic composition typical of the Precambrian.

1. Products characteristic of Phanerozoic bitumens and oils such as waxy alkanes and other plant-derived biomarkers were not detected in concentrations higher than in laboratory procedural blanks. Dinosteranes, detected in trace amounts in the Archean bitumens, are abundant biomarkers in almost all Mesozoic and Cenozoic bitumens (Moldowan et al., 1996). However, lower relative concentrations have also been detected in the Paleozoic and Precambrian (Moldowan et al., 1996), and the oldest known dinosteranes come from the $\sim$1.1-Ga Nonesuch Shale, Michigan (Summons and Walter, 1990). The low relative concentrations of dinosteranes extracted from the Archean rocks (Fig. 10) might indicate a pre-Mesozoic origin.

2. Almost all analyzed Pilbara samples have a high 2α-methylhopane index (C_{31}- MHI) ranging from 8 to 20% (Appendix B, Table A2). C_{31}-MHI measures the abundance of 2α-methyl-$\alpha\beta$-hopane (C_{31}-$\alpha\beta$-Me) relative to C_{30}-$\alpha\beta$-hopane. High values apparently indicate a high cyanobacterial contribution of organic matter (Summons et al., 1999). In the Phanerozoic, cyanobacterial input into marine clastic sediments was commonly low and values for C_{31}-MHI range between $\sim$0 and 9% (Summons et al., 1999). In evaporitic environments, cyanobacterial activity was commonly higher. Therefore, in evaporites and carbonates C_{31}-MHI frequently ranges between 10 and 25%. However, values $>$10% are also typical of Precambrian bitumens from both siliciclastic and evaporitic environments (Summons et al., 1999). Therefore, the high C_{31}-MHI in the Pilbara samples is consistent either with Phanerozoic contamination derived from evaporite or carbonate source rocks or reflects bitumen of Precambrian age. Fortunately, the two possibilities can be distinguished. Oils derived from carbonates and evaporites usually have low concentrations of diasteranes relative to regular sterane (i.e., low Dia/Reg ratios). Clay minerals in siliciclastic rocks, on the other hand, catalyze the conversion of regular steroids into diasteranes, inducing high Dia/Reg ratios (van Kaam-Peters, 1997). In almost all these Pilbara samples, Dia/Reg is very high (Appendix B, Table A2), strongly reducing the probability of contamination by a Phanerozoic oil from a carbonate or evaporite source.

3. In most Phanerozoic marine oils and bitumens, and therefore in most potential recent contaminants, the alkanes *n*-C_{17} and *n*-C_{18} are typically depleted in ^{13}C by 1 to 2‰ relative to pristane and phytane (Logan et al., 1997). In all analyzed Pilbara sampels, on the other hand, the opposite is observed with pristane and phytane depleted in ^{13}C by $\sim$0 to 3‰ relative to the *n*-alkanes. A similar inverted trend is also known for some lacustrine Phanerozoic oils, but is otherwise typical of Precambrian bitumens (Logan et al., 1997). Although the isotopic inversion in the Pilbara samples could be the result of contamination with petroleum products of a lacustrine Phanerozoic origin, the presence of 24-*n*-propylcholestane in the extracts suggests that this is not the case. 24-*n*-propylcholestane in Phanerozoic oils is a specific biomarker for marine environments (Moldowan et al., 1990).

3.5.6. Spatial distribution of hydrocarbons within a rock sample

Syngenetic hydrocarbons and spilled contaminants should have different spatial distributions within a sampled rock. To analyze the depth profile of compounds in the Archean shales, drill core samples were cut into millimeter thick slices and each slice was separately analyzed. The extensive data from these experiments is not the focus of the present study and the results will therefore be discussed in detail elsewhere. However, to allow a full discussion about syngeneity versus contamination, some conclusions are preemptively considered here.

In some drill core samples from the Hamersley and Fortescue Group, hydrocarbons are not homogeneously distributed in their host rock. Saturated and aromatic hydrocarbons of low molecular weight have gradually decreasing concentrations from the center to surfaces of the rock. In contrast, the abundance of higher molecular weight hydrocarbons increases with

distance from the center of the rock. Two models can explain such distributions:

1. Surficial contamination of rock samples by petroleum products and diffusion of hydrocarbons into the pore-space or into fissures, accompanied by in situ chromatographic separation according to molecular mass and subsequent evaporation of lighter compounds from the surface;
2. Escape of indigenous wet-gas from host rocks as the result of pressure release during and after drilling (the "live-oil effect"; Jackson et al., 1986).

It is currently not possible to confirm or reject either model. While surficial contamination appears to be the easier explanation for the observed concentration gradients (Brocks, 2001), only the second explanation, migration of indigenous condensate to the rock surfaces, accounts for the presence of the same overmature, apparently Precambrian bitumen in a set of independent samples derived from different sites at different times. Therefore, more detailed work on spatial hydrocarbon distributions in sedimentary rocks is required for a reliable interpretation of this phenomenon.

3.5.7. Recognition of contamination sources

If the hydrocarbons detected in the Archean shales are recent contaminants, then the contamination source must be ubiquitous and common. The rock samples were collected from eight cores drilled by different companies several hundred kilometers apart, stored at different locations and sampled during several field trips by different workers. Despite this wide range of independent sampling, all rocks contain an overmature, condensate-like hydrocarbon phase with apparently Precambrian characteristics. Thus, unique contamination events such as spillage of petroleum or impregnation from stained sample containers, can be excluded. More common sources of contamination are drilling additives, rock-sawing fluids, organics dissolved in water, and anthropogenic combustion products such as exhausts from diesel engines.

3.5.7.1. Drilling additives.

Most organic additives and lubricants used for diamond drilling cause only minor problems during organic geochemical analysis. However, drillers occasionally use large amounts of highly problematic petroleum based cutting oils and emulsions, particularly when drilling at great depths and through iron ore and chert. Unfortunately, for the cores analyzed in this study, it was not possible to reconstruct the composition of the drilling additives and rod lubricants. However, data from the analysis of the molecular content of millimeter thick slices of core material (section 3.5.6) can rule out drilling additives as a possible contamination source. In a black shale from drill core WRL-1 the highest concentration of the overmature condensate was found beneath a rock surface that was cut after drilling. Therefore, if the hydrocarbons are non-indigenous, then they must have entered the sample after recovery of the core. Moreover, samples *Rae6* from Mt Tom Price and *Rae3* from Mt Whaleback are mine samples and therefore clearly unaffected by drilling additives.

3.5.7.2. Rock-sawing fluids.

Several analyzed Archean drill core samples were not cut with a rock-saw (e.g., *Rae2*) and so cutting fluids are clearly not the source of the hydrocarbons.
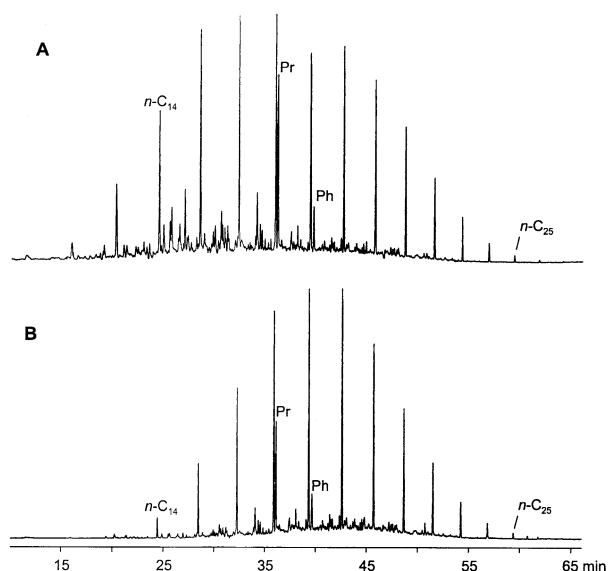

Fig. 14. Gas chromatograms of (A) typical diesel fuel and (B) the solvent extractable component of exhaust of an engine running on the diesel fuel in (A).

3.5.7.3. Organics dissolved in water.

Although drill cores frequently come into contact with water, the aqueous solubility of saturated hydrocarbons is far too low to explain the observed extract yields. GC-MS analysis of diesel-saturated water revealed that the main components are C_1 to C_4-phenols, C_0 to C_3-naphthalenes, C_5 and C_6-benzenes and minor quantities of phenanthrene and methylphenanthrenes. The amount of saturated hydrocarbons soluble in 2 mL of water was below detection limit. Therefore, the saturated hydrocarbons were clearly not carried into the samples in aqueous solution.

3.5.7.4. Diesel fuel and engine exhausts.

Diesel exhausts are ubiquitous in the environment; they have even been detected in glacier-ice at an altitude of 7000 m (Xie et al., 2000). In the Hamersley region, mining equipment consumes many thousand liters of diesel fuel each day (Fig. 14A) and the exhaust products (Fig. 14B) are free to settle on outcrop material and on drill core samples in open core-storage buildings. In the core shed at Mt Tom Price diesel exhausts were detected in dust that had settled on sample-trays of drill core material. Therefore, surficial accumulation of airborne petroleum products on our rock samples is not implausible. However, it is an unlikely source of hydrocarbons in the Pilbara shales:

1. The n-alkane composition of diesel fuel and its exhausts is very different to the detected hydrocarbon composition of the Pilbara rock extracts (except for samples *Tum1* and FVG-1). Light hydrocarbons with 9 to 12 carbon atoms are abundant in most Pilbara samples but are very low in diesel fuel and exhaust (compare Fig. 14B and Fig. 3). Moreover, sterane and hopane biomarkers are commonly much less abundant in diesel fuel than in the samples studied here.
2. Despite the compositional differences of diesel and the Pilbara samples, contaminants may have migrated from the surface into the sample, concentrating lighter components

by in situ fractionation (Brocks, 2001). Quantitative estimates of the amount of diesel required to taint the samples also eliminates this possibility. Typical diesel fuel contains $\sim$0.25 wt.% of n-C_{11} and sample *Roy10* from drill core WRL-1 contains 0.20 μg n-C_{11}/g rock. Eight thousand micrograms of diesel exhausts would have to accumulate on a 100-g piece of rock to account for this n-C_{11} concentration. Similarly, the concentration of n-C_{11} in Mt McRae Shale *Rae2* is 34 μg/g and thus 1.4 g of diesel or diesel exhaust would be required to stain 100 g of the rock. These estimates are conservative, as evaporation of n-C_{11} from the sample surfaces or using n-C_{10} or n-C_9 in the calculation would greatly increase the required minimum values of diesel exhaust contamination. It is highly unlikely that as much as 10 mg/g diesel exhaust came into contact with the Archean rocks.

3. Finally, it is difficult to explain how traces of engine exhausts deposited on rock surfaces, probably mostly adsorbed to soot particles, could have migrated centimeters deep into dense shale without any apparent mobile phase to act as a transportation medium.

3.5.7.5. The unusual composition of Mt McRae shale sample Rae6.

Bitumen *Rae6*, a mine sample from Mt Tom Price, exclusively consists of adamantanes, diamantanes and predominantly unsubstituted PAH. This composition is totally unlike any known source of contamination.

So far it has been argued that the hydrocarbons extracted from Archean rocks are not laboratory artifacts nor contaminants aquired during drilling, cutting, handling or storage. The extracts are thermally overmature, have a condensate-like composition and typical Precambrian characteristics. It is exceedingly unlikely that the wide range of independent Archean samples were all contaminated by anthropogenic petroleum products with the above characteristics. However, it is still possible that the Archean host rocks were adulterated in situ by organic matter from another Precambrian source. In the remaining sections, contamination by circulating ground water, subsurface biologic activity and, most problematic, migrated Precambrian petroleum are considered.

3.5.8. Molecules introduced by circulating ground water or subsurface biologic activity

Subsurface biologic activity or circulating groundwater carrying surficial biolipids might have introduced organic matter into the Archean host rocks. However, the hydrocarbons extracted from all samples clearly have a thermally mature petroleum signature. The rocks have not experienced thermal events after peak metamorphism (2.45–2.0 Ga) capable of turning immature biolipids into highly mature geolipids. Therefore, the extracted hydrocarbons were not derived from post-metamorphic surface or subsurface biota.

3.5.9. Adulteration of Archean rocks by younger migrating petroleum

Petroleum expelled from a younger Precambrian source might have migrated into the Archean terrain and adulterated the sedimentary successions of the Fortescue and Hamersley Group. However, the youngest rocks in the depositional basin belong to the $\sim$2.4-Ga Turee Creek Group and younger petroleum-prone source rocks were never deposited over the top in sufficient thickness for hydrocarbon expulsion to occur. Drill core WRL-1 is located centrally within the craton, at least 150 km from the nearest post-Archean basin, so younger oils migrating laterally would have to travel long distances through deformed and metamorphosed Archean rocks that lack later cross-cutting craton-wide fractures. The sampling area extends from Wittenoom (WRL-1) 200 km to the southeast (DDH324 and DDH257), 100 km to the southwest (G1185-81, B26-7, G906, DE20/74) and 70 km to the northwest (SV-1) (Fig. 1), with further bitumen occurrences of similar composition located 280 km further to the northeast (Eigenbrode et al., 2001). Bitumens were extracted from rocks collected at subsurface depths of $>$ 1800 m in the center of the basin. Therefore, petroleum adulterating the Archean terrain would have to penetrate almost the entire Hamersley Basin and percolate down to great depths. Moreover, bedding-parallel permeability of black shale *Roy3* and pyritic sandstone *Roy4* from WRL-1 was below the detection limit of 0.01 millidarcy. Thus, these rocks have probably been sealed to hydrocarbon migration since they were metamorphosed 2.3 to 2.0 Ga ago. Moreover, the physical mechanisms that could have driven easily adsorbed molecules like polyaromatic hydrocarbons into thick sections of highly compacted, metamorphosed shales remain obscure. Consequently, adulteration of the entire late Archean terrain by overmature Proterozoic petroleum from a source outside the basin is highly unlikely.

3.5.10. Pyrolysis experiments on Archean Kerogens

While it is often difficult to prove that molecules obtained by solvent extraction of rock powder are as old as the host rock, molecular structures that are covalently bound to the kerogen matrix are very likely syngenetic. Therefore, for younger and well-preserved samples, pyrolytic degradation of kerogen is an ideal method of analyzing for indigenous molecules. For most Precambrian kerogens and many overmature samples, however, closed system pyrolytic techniques have not proved to be particularly tractable. As a result, it has not been possible to produce clearly indigenous pyrolysis products from kerogens older than 1.7 Ga (Hoering and Navale, 1987). A comparatively new and potentially more profitable method is hydropyrolysis, a continuous flow technique that degrades polymeric organic matter in a stream of high-pressure hydrogen under the influence of a molybdenum catalyst. In comparison to more conventional pyrolysis techniques, hydropyrolysis is generally distinguished by its efficacy in trace analysis and its high product yields (Love et al., 1995). Hydropyrolysis experiments on Archean kerogens are described in detail by Brocks et al. (in press). Although information about the provenance of aliphatic hydrocarbons and polycyclic biomarkers was not obtained, the hydropyrolysis experiments clearly indicate that at least the aromatic hydrocarbon fraction of shales from the Hamersley Group at Mt Tom Price must be syngenetic (Brocks et al., in press).

4. CONCLUSIONS

4.1. The Arguments for Syngeneity

Three principal sources of contamination must be discounted:

1. hydrocarbons introduced during laboratory procedures;
2. anthropogenic petroleum products introduced during drilling, storage and handling;
3. natural petroleum that was expelled from a younger source and migrated into the Archean terrain.

Procedural blanks run parallel to all samples show that hydrocarbon concentrations obtained by rock extraction are several orders of magnitude higher than the laboratory background level. Moreover, comparison of extract yields from kerogen-rich rocks and kerogen-poor control samples from the same locations indicate that the hydrocarbons were not introduced during sample collection and processing.

Arguments against anthropogenic contamination of drill core samples include the extreme thermal maturity of bitumens from almost all locations, the absence of typical Phanerozoic biomarkers, and the presence of typical Precambrian signatures such as high 2α-methylhopane indices and the inversion of the carbon isotopic relationship between *n*-alkanes and acyclic isoprenoids. Bitumens with these characteristics were discovered in samples from eight different drill cores from depths of 50 to 1800 m depths, drilled by several companies and stored at three different locations several hundred kilometers apart. Moreover, the rocks were collected in 1994, 1996, 1999 and 2000 by different workers and analyzed in two different laboratories. Furthermore, these results were reproduced at Pennsylvania State University on independently sampled material from drill core WRL-1 as well as on additional samples extending the sampling range another 280 km to the east (Eigenbrode et al., 2001). It is exceedingly unlikely that samples from such a wide geographic and stratigraphic range and from so many independent sources were all contaminated by petroleum products showing characteristics typical of Precambrian bitumen and maturities in the wet-gas zone.

Adulteration by a younger Precambrian oil that migrated into the Archean terrain is also unlikely. Younger source rocks are absent in the Hamersley Basin and were never deposited over the top in sufficient thickness for significant hydrocarbon expulsion to occur. Thus, younger petroleum would have had to migrate from the nearest post-Archean basin through at least 150 km of deformed and metamorphosed terrain devoid of cross-cutting craton-wide fractures. Moreover, highly compacted but structurally intact Archean shales were probably sealed to hydrocarbon migration since they were metamorphosed in the Paleoproterozoic. Hence, homogeneous long distance migration of a younger oil into tight Archean rocks over an area of $> 30,000$ km^2 and down to depths of up to 1800 m seems exceedingly unlikely. Moreover, the unusual composition of aromatic hydrocarbons in bitumens from the Mt McRae Shale was also replicated by hydropyrolytic degradation of the kerogens, confirming the syngeneity of these aromatic hydrocarbons.

4.2. The Arguments Against Syngeneity

Characteristics consistent with contamination of the Pilbara samples include the general similarity of the biomarker distribution to those observed in many younger bitumens, the extreme carbon isotopic disparity between some bitumens and kerogens, the absence of saturated hydrocarbons in kerogen pyrolysates, and some maturity parameters for some samples that are too low for the thermal history of the host rocks (especially drill core FVG-1). However, none of these observations (except for the low maturity of FVG-1) are necessarily inconsistent with syngeneity, because plausible alternative explanations not involving contamination exist. More problematic is the survival of complex molecules such as sterane and hopane biomarkers in metamorphosed sediments, a phenomenon that has not previously been demonstrated and a finding that was certainly unexpected. But C_{15+} hydrocarbons have been observed in petroleum reservoirs at present day temperatures $> 200°C$ which suggests that the existence of biomarkers in low-grade matasedimentary rocks ($200–300°C$) is possible. Lastly, the strongly inhomogeneous distribution of the bitumen in individual drill core samples is potentially consistent with surficial staining of the samples and diffusion of hydrocarbons into the rock (Brocks, 2001). The only alternative to contamination involves the operation of a poorly understood mechanism, the 'live-oil effect'. It remains to be seen whether this process could have affected the Hamersley Basin shales.

4.3. Syngeneity vs. Contamination

Although some observations are more easily explained by contamination, the arguments for syngeneity evidently outweigh the objections. Therefore, aliphatic hydrocarbons and biomarkers in bitumens from the Fortescue and Hamersley Groups are regarded as probably syngenetic with their Archean host rocks. Aromatic hydrocarbons, adamantanes and diamantanes from shales of the Hamersley Group at Mt Tom Price and Mt Whaleback are certainly syngenetic, based on their hypermature composition and covalent bonding to kerogen (Brocks et al., in press). These hydrocarbon molecules are therefore 0.8 to 1.1 Ga older than the previously oldest known clearly indigenous bitumen from the McArthur Group, Australia (Jackson et al., 1986). If the polycyclic biomarkers are indeed of Archean age, then a new horizon opens for the understanding of primordial environments and early life on Earth.

Petroleum and Marine Division Trevor Powell. G.A.L. publishes with the permission of the CEO of Geoscience Australia.

Associate editor: R. C. Burruss

REFERENCES

Alexander R., Bastow T. P., Fisher S. J., and Kagi R. I. (1995) Geosynthesis of organic compounds: II. Methylation of phenanthrene and alkylphenanthrenes. *Geochim. Cosmochim. Acta* **59**, 4259–4266.

Anderson K. B. and Muntean J. V (2000) The nature and fate of natural resins in the geosphere. Part X. Structural characteristics of the macromolecular constituents of modern Dammar resin and Class II ambers. *Geochem. Trans.* **1**, paper 1.

Arndt N. T., Nelson D. R., Compston W., Trendall A. F., and Thorne A. M. (1991) The age of the Fortescue Group, Hamersley Basin, Western Australia, from ion microprobe zircon U-Pb results. *Austral. J. Earth Sci.* **38**, *3*, 261–281.

Barghoorn E. S. (1957) Origin of life. *Geol. Soc. Am. Memoir* **67**, 75–85.

Barghoorn E. S., Meinschein W. G., and Schopf J. W. (1965) Paleobiology of a Precambrian shale. *Science* **148**, 461–472.

Barley M. E., Pickard A. L., and Sylvester P. J. (1997) Emplacement of a large igneous province as a possible cause of banded iron formation 2.45 billion years ago. *Nature* **385**, 55–58.

Barley M. E., Pickard A. L., Hagemann S. G., and Folkert S. L. (1999) Hydrothermal origin for the 2 billion year old Mount Tom Price giant iron ore deposit, Hamersley Province, Western Australia. *Mineralium Deposita* **34**, *8*, 784–789.

Blake T. S. (1984) Evidence for stabilization of the Pilbara Block, Australia. *Nature* **307**, 721–723.

Blake T. S. (2001) Cyclic continental mafic tuff and flood basalt volcanism in the late Archean Nullagine and Mount Jope supersequences in the eastern Pilbara, Western Australia. *Precam. Res.* **107**, *3–4*, 139–177.

Blake T. S. and Barley M. E. (1992) Tectonic evolution of the late Archaean to Early Proterozoic Mount Bruce Megasequence Set, Western Australia. *Tectonics* **11**, *6*, 1415–1425.

Boreham C. J., Crick I. H., and Powell T. G. (1988) Alternative calibration of the Methylphenanthrene Index against vitrinite reflectance: Application to maturity measurements on oils and sediments. *Org. Geochem.* **12**, *3*, 289–294.

Bradshaw M. T., Bradshaw J., Murray A. P., Needham D. J., Spencer L., Summons R. E., Wilmot J., and Winn S. (1994) Petroleum systems in western Australian basins. In *The Sedimentary Basins of Western Australia. Proceedings of the West Australian Basins Symposium*, pp. 93–118.

Brigaud F. (1998) *HP-HT Petroleum System Prediction From Basin to Prospect Scale.* Final report, project OG/211/94FR/UK. Commission of the European Community, Directorate General for Energy, Brussels.

Brocks J. J (2001) *Molecular Fossils in Archean Rocks.* Ph.D. dissertation, University of Sydney.

Brocks J. J., Logan G. A., Buick R., and Summons R. E. (1999) Archean molecular fossils and the early rise of eukaryotes. *Science* **285**, 1033–1036.

Brocks J. J., Buick R., Summons R. E., and Logan G. A. (2003) A reconstruction of Archean biological diversity based on molecular fossils from the 2.78 to 2.45 billion-year-old Mount Bruce Supergroup, Hamersley Basin, Western Australia. *Geochim. Cosmochim. Acta* **67**, 4321–4335.

Brocks J. J., Love G. D., Snape C. E., Logan G. A., Summons R. E., and Buick R. (2003) Release of bound aromatic hydrocarbons from late Archean and Mesoproterozoic kerogens via hydropyrolysis. *Geochim. Cosmochim. Acta* **67**(8), 1521–1530.

Buick R. (1992) The antiquity of oxygenic photosynthesis: Evidence from stromatolites in sulphate-deficient Archaean lakes. *Science* **255**, 74–77.

Buick R., Thornett J. R., McNaughton N. J., Smith J. B., Barley M. E., and Savage M. (1995) Record of emergent continental crust ∼3.5 billion years ago in the Pilbara Craton of Australia. *Nature* **375**, 574–577.

Burnham A. K., Gregg H. R., Ward R. L., Knauss K. G., Copenhaver S. A., Reynolds J. G., and Sanborn R. (1997) Decomposition kinetics and mechanism of n-hexadecane-1,2-$^{13}C_2$ and dodec-1-ene-1,2-$^{13}C_2$ doped in petroleum and n-hexadecane. *Geochim. Cosmochim. Acta* **61**, 3725–3737.

Chen J., Fu J., Sheng G., Liu D., and Zhang J. (1996) Diamondoid hydrocarbon ratios: Novel maturity indices for highly mature crude oils. *Org. Geochem.* **25**, *3/4*, 179–190.

Dahl J. E., Moldowan J. M., Peters K. E., Claypool G. E., Rooney M. A., Michael G. E., Mello M. R., and Kohnen M. L. (1999) Diamondoid hydrocarbons as indicators of natural oil cracking. *Nature* **399**, 54–57.

Dominé F., Bounaceur R., Scacchi G., Marquaire P.-M., Dessort D., Pradier B., and Brevart O. (2002) Up to what temperature is petroleum stable? New insights from a 5200 free radical reaction model. *Org. Geochem.* **33**, 1487–1499.

Eigenbrode J. L., Freeman K. H., Brocks J. J., Summons R. E., and Logan G. A. (2001) Late Archean biomarkers of carbonate and shale lithologies from the Hamersley Basin, Pilbara Craton, Western Australia. *Eleventh Ann. V. M. Goldschmidt Conference.*

Espitalié J., Laporte J. L., Madec M., Marquis F., Leplat P., Paulet J., and Boutefeu A. (1977) Methode rapide de characterisation des roches meres, de leur potentiel petrolier et de leur degre d'evolution. *Revue de l'Institut Français du Pétrole* **32**, *1*, 23–42.

Fiebiger W. (1973) *Organische Substanzen in Präkambrischen Itabiriten und Deren Nebengesteinen. Ein Beitrag zur Deutung der Itabiritgenese.* Ph.D. dissertation, Johannes Gutenburg Universität zu Mainz.

Frey M., de Capitani C., and Liou J. G. (1991) A new petrogenetic grid for low-grade metabasites. *J. Metamorphic Geol.* **9**, *1*, 497–509.

George S. C. (1992) Effect of igneous intrusion on the organic geochemistry of a siltstone and an oil shale horizon in the Midland Valley of Scotland. *Org. Geochem.* **18**, *5*, 705–723.

Goodarzi F., Brooks P. W., and Embry A. F. (1989) Regional maturity as determined by organic petrography and geochemistry of the Schei Point Group (Triassic) in the western Sverdrup Basin, Canadian Arctic Archipelago. *Mar. Petrol. Geol.* **6**, *4*, 290–302.

Gressier J. M. (1996) *The Transition Between the Fortescue and Hamersley Groups in the Nullagine Synclinorium, Western Australia: Implications for Late Archaean Evolution of the Pilbara Craton.* B.Sc. (Hons) thesis, University of Sydney.

Han J. and Calvin M. (1969) Occurrence of fatty acids and aliphatic hydrocarbons in a 3.4 billion-year-old sediment. *Nature* **224**, 576–577.

Harmsworth R. A., Kneeshaw M., Morris R. C., Robinson C. J., Shrivastava P. K. (1990) BIF-derived iron ores of the Hamersley Province. In *Geology of the Mineral Deposits of Australia and Papua New Guinea* (ed. F. E. Hughes), pp. 617–642. The Australasian Institute of Mining and Metallurgy.

Hayes J. M., Kaplan I. R., and Wedeking K. W. (1983) Precambrian organic geochemistry, preservation of the record. In *Earth's Earliest Biosphere, Its Origin and Evolution* (ed. J. W. Schopf), pp. 93–134. Princeton University Press, Princeton, NJ.

Hoering T. C. (1965) The extractable organic matter in Precambrian rocks and the problem of contamination. *Carnegie Inst. Wash. Yearbook* **64**, 215–218.

Hoering T. C. (1966) Criteria for suitable rocks in Precambrian organic geochemistry. *Carnegie Inst. Wash. Yearbook* **65**, 365–372.

Hoering T. C. (1967) The organic geochemistry of Precambrian rocks. In *Researches in Geochemistry, Vol. 2* (ed. P. H. Abelson), pp. 87–111. John Wiley, New York.

Hoering T. C. and Navale V. (1987) A search for molecular fossils in the kerogen of Precambrian sedimentary rocks. *Precam. Res.* **34**, *3–4*, 247–267.

Höld I. M., Schouten S., Jellema J., and Sinninghe Damsté J. S. (1999) Origin of free and bound mid-chain methyl alkanes in oil, bitumens and kerogens of the marine, Infracambrian Huqf Formation (Oman). *Org. Geochem.* **30**, 1411–1428.

Imbus S. W. and McKirdy D. M. (1993) Organic geochemistry of Precambrian sedimentary rocks. In *Organic Geochemistry* (eds. M. H. Engel and S. A. Macko), pp. 657–684. Plenum Press, New York.

Jackson M. J., Powell T. G., Summons R. E., and Sweet I. P. (1986) Hydrocarbon shows and petroleum source rocks in sediments as old as 1.7 billion years. *Nature* **322**, 727–729.

Jinggui L., Philp P., and Mingzhong C. (2000) Methyl diamantane index (MDI) as a maturity parameter for lower Palaeozoic carbonate rocks at high maturity and overmaturity. *Org. Geochem.* **31**, 267–272.

Kennard J. M., Jackson M. J., Romine K. K., Shaw R. D., and Southgate P. N. (1994) Depositional sequences and associated petroleum systems of the Canning Basin, WA. *The Sedimentary Basins of Western Australia, Proceedings of Petroleum Exploration Society of Australia Symposium*, pp. 657–676.

Klein C. and Gole M. J. (1981) Mineralogy and petrology of parts of the Marra Mamba Iron Formation, Hamersley Basin, Western Australia. *Am. Mineral.* **66**, *5–6*, 507–525.

Knott D (1999) Elf U.K. expands HP-HT expertise with Elgin-Franklin development. *Oil Gas J.* June 21, pp. 18–22.

Krapez B. (1993) Sequence stratigraphy of the Archaean supracrustal belts of the Pilbara Block, Western Australia. *Precam. Res.* **60**, 1–45.

Kvenvolden K. A. and Hodgson G. W. (1969) Evidence for porphyrins in early Precambrian Swaziland system sediments. *Geochim. Cosmochim. Acta* **33**, 1195–1202.

Logan G. A., Hayes J. M., Hieshima G. B., and Summons R. E. (1995) Terminal Proterozoic reorganisation of biogeochemical cycles. *Nature* **376**, 53–56.

Logan G. A., Summons R. E., and Hayes J. M. (1997) An isotopic biogeochemical study of Neoproterozoic and Early Cambrian sediments from the Centralian Superbasin, Australia. *Geochim. Cosmochim. Acta* **61**, 5391–5409.

Logan G. A., Calver C. R., Gorjan P., Summons R. E., Hayes J. M., and Walter M. R. (1999) Terminal Proterozoic mid-shelf benthic microbial mats in the Centralian Superbasin and their environmental significance. *Geochim. Cosmochim. Acta* **63**, 1345–1358.

Love G. D., Snape C. E., Carr A. D., and Houghton R. C. (1995) Release of covalently-bound alkane biomarkers in high yields from kerogen via catalytic hydropyrolysis. *Org. Geochem.* **23**, *10*, 981–986.

Mackenzie A. S., Hoffmann C. F., and Maxwell J. R. (1981) Molecular parameters of maturation in the Toarcian shales, Paris Basin, France—III. Changes in aromatic steroid hydrocarbons. *Geochim. Cosmochim. Acta* **45**, 1345–1355.

Martin D. M., Li Z. X., Nemchin A. A., and Powell C. M. (1998) A pre-2.2 Ga age for giant hematite ores of the Hamersley Province, Australia? *Econ. Geol.* **93**, *7*, 1084–1090.

McCaffrey M. A., Moldowan J. M., Lipton P. A., Summons R. E., Peters K. E., Jeganathan A., and Watt D. S. (1994) Paleoenvironmental implications of novel C_{30} steranes in Precambrian to Cenozoic age petroleum and bitumen. *Geochim. Cosmochim. Acta* **58**, 529–532.

McKirdy D. M. (1974) Organic geochemistry in Precambrian research. *Precam. Res.* **1**, *2*, 75–137.

McNeil R. I. and BeMent W. O. (1996) Thermal stability of hydrocarbons: Laboratory criteria and field examples. *Energy Fuels* **10**, 60–67.

Meinschein W. G. (1965) Soudan Formation: organic extracts of early Precambrian rocks. *Science* **150**, 601–605.

Mello M. R., Koutsoukos E. A. M., Hart M. B., Brassel S. C., and Maxwell J. R. (1989) Late Cretaceous anoxic events in the Brazilian continental margin. *Org. Geochem.* **14**, *5*, 529–542.

Moldowan J. M., Fago F. J., Lee C. Y., Jacobson S. R., Watt D. S., Slougui N.-E., Jeganathan A., and Young D. C. (1990) Sedimentary 24-*n*-propylcholestanes, molecular fossils diagnostic of marine algae. *Science* **247**, 309–312.

Moldowan J. M., Fago F. J., Carlson R. M. K., Young D. C., Van Duyne G., Clardy J., Schoell M., Pillinger C. T., and Watt D. S. (1991) Rearranged hopanes in sediments and pretroleum. *Geochim. Cosmochim. Acta* **55**, 3333–3353.

Moldowan J. M., Dahl J., Jacobson S. R., Huizinga B. J., Fago F. J., Shetty R., Watt D. S., and Peters K. E. (1996) Chemostratigraphic reconstruction of biofacies: Molecular evidence linking cyst-forming dinoflagellates with pre-Triassic ancestors. *Geology* **24**, *2,* 159–162.

Morris R. C. (1993) Genetic modelling for banded iron-formation of the Hamersley Group, Pilbara Craton, Western Australia. *Precam. Res.* **60**, *1–4,* 243–286.

Morris R. C. and Horwitz R. C. (1983) The origin of the iron-formation-rich Hamersley Group of Western Australia—Deposition on a platform. *Precam. Res.* **21**, *3/4,* 273–297.

Nagy B. (1970) Porosity and permeability of the early Precambrian Onverwacht chert: Origin of the hydrocarbon content. *Geochim. Cosmochim. Acta* **34**, 525–526.

Nagy B. and Nagy L. A. (1969) Early Pre-Cambrian Onverwacht microstructures: Possibly the oldest fossils on Earth? *Nature* **223**, 1226–1229.

Oehler J. H. (1977) Irreversible contamination of Precambrian kerogen by ^{14}C-labelled organic compounds. *Precam. Res.* **4**, *3,* 221–227.

Pepper A. S. and Dodd T. A. (1995) Simple kinetic models of petroleum formation. Part II: Oil-gas cracking. *Mar. Petrol. Geol.* **12**, *3,* 321–340.

Perkins G. M., Bull I. D., Ten Haven H. L., Rullkötter J., Smith Z. E. F., and Peakman T. M. (1995) First positive identification of triterpanes of the taraxastane family in petroleums and oil shales: 19a(H)-taraxastane and 24-nor-19a(H)-taraxastane. Evidence for a previously unrecognised diagenetic alteration pathway of lup-20(29)-ene derivatives. *17th International Meeting on Organic Geochemistry. Organic Geochemistry: Developments and Applications to Energy, Climate, Environments and Human History*, pp. 247–279.

Peters K. E. and Moldowan J. M. (1993) *The Biomarker Guide*. Prentice Hall, New York.

Peters K. E., Moldowan J. M., and Sundararaman P. (1990) Effects of hydrous pyrolysis on biomarker thermal maturity parameters: Monterey phosphatic and siliceous members. *Org. Geochem.* **15**, *3,* 249–265.

Price L. C. (1993) Thermal stability of hydrocarbons in nature: limits, evidence, characteristics, and possible controls. *Geochim. Cosmochim. Acta* **57**, 3261–3280.

Price L. C. (1997) Minimum thermal stability levels and controlling parameters of methane, as determined by C_{15+} hydrocarbon thermal stabilities. In *Geologic Controls of Deep Natural Gas Resources in the United States, Vol. 2146-K* (eds. T. S. Dyman, D. D. Rice, and P. A. Westcott), pp. 139–176.

Price L. C. (2000) Organic metamorphism in the California petroleum basins: Chap. B—Insights from extractable bitumen and saturated hydrocarbons. *U.S. Geol. Survey Bull.* **B 2174-B**.

Püttmann W., Hagemann H. W., Merz C., and Speczik S. (1988) Influence of organic material on mineralization processes in the Permian Kupferschiefer Formation, Poland. *Org. Geochem.* **13**, *1–3,* 357–363.

Radke M., Welte D. H., and Willsch H. (1982a) Geochemical study on a well in the western Canada Basin: Relation of the aromatic distribution pattern to maturity of organic matter. *Geochim. Cosmochim. Acta* **46**, 1–10.

Radke M., Willsch H., Leythaeuser D., and Teichmueller M. (1982b) Aromatic components of coal: Relation of distribution pattern to rank. *Geochim. Cosmochim. Acta* **46**, 1831–1848.

Radke M., Welte D. H., and Willsch H. (1986) Maturity parameters based on aromatic hydrocarbons: Influence of the organic matter type. *Org. Geochem.* **10**, *1–3,* 51–63.

Rasmussen B., Fletcher I. R., and McNaughton N. J. (2001) Dating low-grade metamorphic events by SHRIMP U-Pb analysis of monazite in shales. *Geology* **29**, *10,* 963–966.

Raymond A. C. and Murchison D. G. (1992) Effect of igneous activity on molecular-maturation indices in different types of organic matter. *Org. Geochem.* **18**, *5,* 725–735.

Riolo J., Hussler G., Albrecht P., and Connan J. (1985) Distribution of aromatic steroids in geological samples: Their evaluation as geochemical parameters. *Org. Geochem.* **10**, *4–6,* 981–990.

Rutten M. G. (1971) *The Origin of Life by Natural Causes*. Elsevier, New York.

Sajgó C. (2000) Assessment of generation temperatures of crude oils. *Org. Geochem.* **31**, *12,* 1301–1323.

Sanyal S. K., Kvenvolden K. A., and Marsden S. S. J. (1971) Permeabilities of Precambrian Onverwacht cherts and other low permeability rocks. *Nature* **232**, 325–327.

Sieskind O., Joly G., and Albrecht P. (1979) Simulation of the geochemical transformation of sterols: Superacid effect of clay minerals. *Geochim. Cosmochim. Acta* **43**, 1675–1680.

Simoneit B. R. T. (1993) Hydrothermal activity and its effects on sedimentary organic matter. In *Bitumen in Ore Deposits* (eds. J. Parnell, H. Kucha, and P. Landais), pp. 81–95. Springer-Verlag, New York.

Smith R. E., Perdrix J. L., and Parks T. C. (1982) Burial metamorphism in the Hamersley Basin, Western Australia. *J. Petrol.* **23**, *1*, 75–102.

Sofer Z. (1980) Preparation of carbon dioxide for stable carbon isotope analysis of petroleum fractions. *Anal. Chem.* **52**, 1389–1391.

Summons R. E. and Walter M. R. (1990) Molecular fossils and microfossils of prokaryotes and protists from Proterozoic sediments. *Am. J. Sci.* **290-A**, 212–244.

Summons R. E. and Jahnke L. L. (1992) Hopenes and hopanes methylated in ring-A: Correlation of the hopanoids from extant methylotrophic bacteria with their fossil analogues. In *Biological Markers in Sediments and Petroleum* (eds. J. M. Moldowan, P. Albrecht, and R. P. Philp), pp. 182–200. Prentice Hall, New York.

Summons R. E., Volkman J. K., and Boreham C. J. (1987) Dinosterane and other steroidal hydrocarbons of dinoflagellate origin in sediments and petroleum. *Geochim. Cosmochim. Acta* **51**, 3075–3082.

Summons R. E., Powell T. G., and Boreham C. J. (1988) Petroleum geology and geochemistry of the Middle Proterozoic McArthur Basin, northern Australia: III. Composition of extractable hydrocarbons. *Geochim. Cosmochim. Acta* **52**, 1747–1763.

Summons R. E., Thomas J., Maxwell J. R., and Boreham C. J. (1992) Secular and environmental constraints on the occurrence of dinosterane in sediments. *Geochim. Cosmochim. Acta* **56**, 2437–2444.

Summons R. E., Jahnke L. L., Hope J. M., and Logan G. A. (1999) 2-Methylhopanoids as biomarkers for cyanobacterial oxygenic photosynthesis. *Nature* **400**, 554–557.

Taylor D., Dalstra H. J., Harding A. E., Broadbent G. C., and Barley M. E. (2001) Genesis of high-grade hematite orebodies of the Hamersley Province, Western Australia. *Econ. Geol.* **96**, *4*, 837–873.

Thompson K. F. M. (1987) Fractionated aromatic petroleums and the generation of gas condensates. *Org. Geochem.* **11**, *6*, 573–590.

Thompson K. F. M. (1988) Gas-condensate migration and oil fractionation in deltaic systems. *Mar. Petrol. Geol.* **5**, *3*, 237–246.

Trendall A. F., Nelson D. R., de Laeter J. R., and Hassler S. W. (1998) Precise zircon U-Pb ages from the Marra Mamba Iron Formation and Wittenoom Formation, Hamersley Group, Western Australia. *Austral. J. Earth Sci.* **45**, 137–142.

van Aarssen B. G. K., Cox H. C., Hoogendoorn P., and de Leeuw J. W. (1990) A cadinene biopolymer in fossil and extant dammar resins as a source for cadinanes and bicadinanes in crude oils from South East Asia. *Geochim. Cosmochim. Acta* **54**, 3021–3031.

van Kaam-Peters H. M. E. (1997) *The Depositional Environment of Jurassic Organic-Rich Sedimentary Rocks in NW Europe. A Biomarker Approach.* Ph.D. dissertation, University of Utrecht.

Wontka J. F. (1979) *Organisch-Geochemische Untersuchungen an Präkambrischen Stromatolithen-Kalken und Deren Nebengesteinen.* Ph.D. dissertation, Johannes Gutenburg Universität zu Mainz.

Woodring W. P. (1954) Conference on biochemistry, paleoecology, and evolution. *Proc. Nat. Acad. Sci.* **40**, 219–224.

Xie S., Yao T., Kang S., Xu B., Duan K., and Thompson L. G. (2000) Geochemical analysis of a Himalayan snowpit profile: implications for atmospheric pollution and climate. *Org. Geochem.* **31**, 15–23.

Zhusheng J., Philp R. P., and Lewis C. A. (1988) Fractionation of biological markers in crude oils during migration and the effects on correlation and maturation parameters. *Org. Geochem.* **13**, *1–3*, 561–571.

APPENDIX

STRATIGRAPHY OF THE FORTESCUE AND HAMERSLEY GROUPS

A.1. Fortescue Group

Deposition of the Fortescue Group, predominantly consisting of flood basalts with intercalated clastic, carbonate and tuffaceous sediments, was initiated at ~2.775 Ga (Arndt et al., 1991; Blake, 2001). The group has been divided into six lithostratigraphic formations, four

Table A1. Simplified stratigraphy of the Pilbara Craton and surrounding areas. Geochronological data is in million years (Ma).

			Formation (Fm)	Member (Mm)	Age
Paleoproterozoic	Mount Bruce Supergroup	Wyloo Group			
		Turee Creek Group			
		Hamersley Group	Boolgeeda Iron Fm		2449 ±3[a]
			Woongarra Volcanics		
			Weeli Wolli Fm		
			Brockman Iron Fm	Yandicoogina Shale	2470 ±4[b]
				Joffre Mm	
				Whaleback Shale ★	
				Dales Gorge Mm ★	
Archean			Mt McRae Shale ★		
			Mt Sylvia Fm		
			Wittenoom Dolomite		2561 ± 8[c]
			Marra Mamba Iron Fm	Mt Newman Mm	2597 ± 5[c]
				McLeod Mm ★	
				Nammuldi Mm ★	
		Fortescue Group	Jeerinah Fm	Roy Hill Shale ★	2690 ± 16[d]
				Warrie Mm ★	2715 ± 2[e]
			Maddina Basalt ★		2718 ± 2[e]
			Tumbiana Fm ★		2724 ±5[e]
			Kylena Basalt		2741 ± 3[e]
			Hardey Fm ★		2765 ± 4[e]
			Mount Roe Basalt		2775 ± 10[d]
		Pilbara Supergroup			2850[f]
					3515 ± 3[g]

[a] Barley et al. (1997); [b] Blake and Barley (1992); [c] Trendall et al. (1998); [d] Arndt et al. (1991); [e] Blake et al. (unpublished results.); [f] Krapez (1993); [g] Buick et al. (1995).
★ Units analyzed in this study.

of which were sampled (Appendix B, Table A1). In general, deposition of all but the topmost Jeerinah Formation was probably non-marine in the northern part of the Craton, but was entirely marine in the south. The tectonic setting for deposition was epicratonic, in half-grabens formed during two stages of rifting (Blake, 1984).

The predominantly fluvial **Hardey Formation** unconformably overlies the Mount Roe Basalt. In the West Pilbara subbasin, where drillholes WRL-1 and SV-1 are located, the lower section of the Hardey Formation is up to 1500 m thick and dominated by terrigenous and volcanoclastic sedimentary rocks. This sequence is overlain by a complex sedimentary unit with 100 to 250 m of mudstones (sample *Har1*), sandstones and conglomerates interbedded with abundant tuff horizons. In the West Pilbara subbasin the **Tumbiana Formation** has a thickness of up to 320 m, consisting of interbedded basalt, pyroclastic and reworked tuff with subordinate stromatolitic carbonate, terrigenous sandstone and massive kerogenous mudstone (sample *Tum1*) (Buick, 1992). The unit was apparently deposited in alluvial fan settings and fluvial and lacustrine environments which were frequently evaporitic and desiccated (Buick, 1992). On the northern part of the craton, the **Maddina Basalt** consists of ~1000 m of mainly subaerial flood basalt (*Mad1*) with subordinate tuff, sandstone and mudstone.

The sedimentary **Jeerinah Formation** unconformably overlies the Maddina Basalt (Gressier, 1996) and is subdivided into the Warrie Member and the Roy Hill Shale. In drill core WRL-1 the **Warrie Member** has a total thickness of ~64 m. The basal unit is a ~1 m thick, kerogen-rich massive mudstone (*War1*), overlain by interbedded units of moderately pyritic and highly kerogenous massive mudstone (*War2* and *War5*), graded or rippled sandstone and siltstone, green and translucent plane-bedded chert, tuff and calcarenite. Based on ripple mark morphology, Gressier (1996) suggested that the Warrie Member was deposited in a shallow marine environment.

The **Roy Hill Shale Member** is distinguished from the unconformably underlying Warrie Member by a lower content of carbonates and a higher content of sulfides. The Roy Hill Shale in drill core WRL-1 has a thickness of 37 m and is overwhelmingly dominated (97%) by kerogenous to highly kerogenous, massive to weakly plane-laminated mudstones containing abundant pyrite laminae and chert pods (*Roy1–Roy11*) (chert pods are a soft sediment deformation feature common in Australian BIFs that structurally resemble pinch-and-swell structures in igneous veins in metamorphic rocks). Based on the absence of bedforms, Gressier (1996) suggested that the Roy Hill Shale was deposited

Table A2. Biomarker ratios.

	Hopanes[a]							Steranes[b]	
	C27/ C29	C29/ C30	C30/ C31	Ts/ Ts + Tm	C29Ts/ C29	C31S/ (S + R)	C31 MHI	Ster/Hop	Dia/Reg
Hamersley Group									
Tom Price area									
Dal1	0.72	1.4	1.1	0.51	0.16	0.56	8.0	82	0.36
*Dal2**	*0.51*[c]	*1.5*	*1.1*	*0.57*	*0.27*	*0.61*	*11*	*0.71*	*0.54*
Rae1	1.2	1.2	1.4	0.44	0.19	0.58	8.6	1.99	0.56
Rae2	0.74	1.7	1.2	0.38	0.12	0.56	10	1.43	0.70
Rae6	—	—	—	—	—	—	—	—	—
Bee1	0.51	1.7	1.0	0.40	0.12	0.58	12	0.57	0.40
Mt Whaleback Mine									
Wal2	1.6	1.0	1.5	0.64	0.13	0.61	11	1.55	0.80
Rae3	*0.61*	*1.3*	*1.7*	*0.55*	*0.21*	*0.58*	*7.6*	*1.52*	*1.00*
Rae5	0.61	2.2	1.1	0.61	0.15	0.60	20	0.71	0.73
Wittenoom									
*Wal1**	*0.78*	*0.85*	*2.2*	*0.42*	*0.33*	*0.58*	*3.5*	*1.89*	*0.64*
*Rae4**	*0.66*	*1.3*	*1.2*	*0.43*	*0.19*	*0.62*	*8.0*	*0.57*	*0.36*
Mam3*	0.68	1.8	1.2	0.56	0.22	0.56	14	0.62	0.56
Mam2	0.72	1.3	1.0	0.58	0.17	0.57	7.3	0.67	0.70
Mam1	1.3	1.3	1.1	0.59	0.23	0.58	13	0.79	0.58
Fortescue Group									
Roy1	1.1	1.3	1.3	0.57	0.24	0.56	12	0.95	0.91
Roy10	1.1	1.7	1.5	0.57	0.21	0.57	11	1.19	1.04
Roy2	0.57	2.1	1.5	0.59	0.16	0.61	17	2.59	1.33
Roy11	1.1	1.6	1.7	0.58	0.16	0.57	11	1.24	0.93
Roy3	1.3	1.4	1.5	0.58	0.17	0.56	12	1.13	0.87
War5	0.96	1.7	1.4	0.56	0.12	0.59	10	1.08	0.99
*War1**	*1.2*	*1.3*	*1.3*	*0.62*	*0.26*	*0.57*	*10*	*0.70*	*0.57*
*Mad1**	*1.2*	*1.2*	*1.3*	*0.59*	*0.25*	*0.57*	*11*	*0.78*	*0.43*
Har1	0.67	1.8	1.5	0.51	0.12	0.57	11	1.03	0.70
FVG1	0.84	1.4	1.5	0.56	0.20	0.56	7.4	0.99	0.92
FVG2	0.55	1.4	1.4	0.57	0.25	0.56	13	0.85	0.58
War2	*1.2*	*1.1*	*1.6*	*0.58*	*0.27*	*0.59*	*8.4*	*1.00*	*0.43*
Tum1	*0.74*	*1.4*	*1.1*	*0.59*	*0.26*	*0.56*	*13*	*0.40*	*0.50*

[a] **Hopane** biomarker ratios were measured using uncorrected MRM $M^+ \to 191$ and $M^+ \to 205$ transitions relative to D_4 as internal standard and are defined as follows (compound abbreviations as defined in the text): **C27/C29** = $(Ts + Tm)/C_{29}\text{-}\alpha\beta$; **C29/C30** = $C_{29}\text{-}\alpha\beta/C_{30}\text{-}\alpha\beta$; **C30/C31** = $C_{30}\text{-}\alpha\beta/(C_{31}\text{-}\alpha\beta\text{-}22S + C_{31}\text{-}\alpha\beta\text{-}22R)$; **C29Ts/C29** = $C_{29}Ts/C_{29}\text{-}\alpha\beta$; **C31S/(S + R)** = $C_{31}\text{-}\alpha\beta\text{-}22S/(C_{31}\text{-}\alpha\beta\text{-}22S + C_{31}\text{-}\alpha\beta\text{-}22R)$; **C31 MHI** (2$\alpha$-Methylhopane Index) = $C_{31}\text{-}2\alpha\text{-}Me/(C_{31}\text{-}2\alpha\text{-}Me + C_{30}\text{-}\alpha\beta)$.

[b] **Sterane** biomarker ratios were measured using uncorrected MRM $M^+ \to 217$ transitions relative to D_4 as internal standard and are defined as follows (compound abbreviations as defined in the text): **Ster/Hop** = (Σ C_{27} to C_{29} $\alpha\alpha\alpha$ and $\alpha\beta\beta$-steranes and $\beta\alpha$-diasteranes)/(Σ hopanes Ts, Tm, $C_{29}\text{-}\alpha\beta$, $C_{29}Ts$, $C_{30}\text{-}\alpha\beta$, $C_{31}\text{-}\alpha\beta\text{-}22[S + R]$, $C_{31}\text{-}2\alpha\text{-}Me$); **Dia/Reg** = ($\Sigma$ C_{27} to C_{29} $\beta\alpha$-diasteranes)/(Σ C_{27} to C_{29} $\alpha\alpha\alpha$ and $\alpha\beta\beta$-steranes); **C27S/(S + R)** = $C_{27}\text{-}\alpha\alpha\alpha\text{-}20S/(C_{27}\text{-}\alpha\alpha\alpha\text{-}20S + C_{27}\text{-}\alpha\alpha\alpha\text{-}20R)$ (C28S/[S + R] and C29S/[S + R] are defined according to C27S/[S + R]); **C27$\beta\beta$/($\alpha\alpha$ + $\beta\beta$)** = $(C_{27}\text{-}\alpha\beta\beta\text{-}20S + C_{27}\text{-}\alpha\beta\beta\text{-}20R)/(C_{27}\text{-}\alpha\beta\beta\text{-}20S + C_{27}\text{-}\alpha\beta\beta\text{-}20R + C_{27}\text{-}\alpha\alpha\alpha\text{-}20S + C_{27}\text{-}\alpha\alpha\alpha\text{-}20R)$ (C28$\beta\beta$/$\alpha\alpha$ + $\beta\beta$ and C29$\beta\beta$/($\alpha\alpha$ + $\beta\beta$) are defined according to C27$\beta\beta$/($\alpha\alpha$ + $\beta\beta$); Regular sterane distribution **RegC27%** = (C_{27} $\alpha\alpha\alpha\text{-}20$ [S + R] and $\alpha\beta\beta\text{-}20$ [S + R]) / (Σ C_{27} to C_{29} $\alpha\alpha\alpha\text{-}20$ [S + R] and $\alpha\beta\beta\text{-}20$ [S + R]) (RegC28% and RegC29% are defined according to RegC27%); Diasterane distribution **DiaC27%** = $(C_{27}\text{-}\beta\alpha\text{-}20$ [S + R])/(Σ C_{27} to $C_{29}\text{-}\beta\alpha\text{-}20[S + R]$) (DiaC28% and DiaC29% are defined according to DiaC27%).

[c] Values printed in italics indicate possibly unreliable data with low extract/blank ratios (see laboratory procedural blanks in section 3.5.1.).

* = Kerogen-free or kerogen-poor control samples (blank samples). '—' = not detected.

in a marine low-energy environment below storm wave base. The Roy Hill Shale conformably grades into the overlying Hamersley Group, a transition marked by a gradual decrease in shale units and an increase in chert bands.

A.2. Hamersley Group

The Hamersley Group is up to 2.5 km thick and is dominated by oxide facies BIF, dolostone and shale. BIF deposition extends over an area of at least 60,000 km² with remarkable lateral stratigraphic continuity. Coarse terrigenous clastic sediments are almost completely absent (Morris, 1993). The Hamersley Group is also host to some of the world's biggest iron ore deposits. Samples from the Mt McRae Shale and Brockman Iron Formation were collected from shale closely associated or interbedded with iron ore in mines at Tom Price (Mt Tom Price) and Newman (Mt Whaleback).

Based on lithostratigraphy, the Hamersley Group is divided into

eight formations (Appendix B, Table A1). The 2.597-Ga **Marra Mamba Iron Formation** (Trendall et al., 1998) has a maximum regional thickness of 230 m (Klein and Gole, 1981) and consists of two BIF-rich members separated by a more shaley sequence. The basal **Nammuldi Member** is predominantly composed of coarsely podded bands of sulfidic and oxidic chert-BIF interbedded with bands of highly ferruginous and kerogen-rich massive mudstone (*Mam1* and *Mam2*) (Morris, 1993). The overlying **McLeod Member** is characterized by a higher proportion of shale. Shale bands are of centimeter to meter thickness, are dominated by stilpnomelane and chlorite with large amounts of pyrite, pyrrhotite, hematite and siderite (*Mam3*) and were probably formed by a combination of chemical and pyroclastic deposition (Morris, 1993). Morris (1993) suggested that the Marra Mamba Iron Formation was deposited on either side of a narrow carbonate bank, which grew into a large shallow-marine carbonate platform during formation of the conformably overlying Wittenoom Dolomite.

	C27 S/(S + R)	C28 S/(S + R)	C29 S/(S + R)	C27 ββ/ (αα + ββ)	C28 ββ/ (αα + ββ)	C29 ββ/ (αα + ββ)	Reg C27 (%)	Reg C28 (%)	Reg C29 (%)	Dia C27 (%)	Dia C28 (%)	Dia C29 (%)
						Steranes[b] (continued)						
Hamersley Group												
Tom Price area												
Dal1	0.41	0.55	0.52	0.35	0.49	0.52	54	20	25	54	25	22
*Dal2**	*0.54*	*0.55*	*0.44*	*0.47*	*0.52*	*0.51*	*41*	*30*	*29*	*44*	*31*	*25*
Rae1	0.52	0.66	0.70	0.51	0.61	0.61	51	25	24	48	29	23
Rae2	0.47	0.63	0.58	0.49	0.61	0.59	58	19	23	62	24	15
Rae6	—	—	—	—	—	—	—	—	—	—	—	—
Bee1	0.44	0.69	0.67	0.42	0.58	0.59	50	18	32	53	23	24
Mt Whaleback Mine												
Wal2	0.60	0.72	0.72	0.58	0.64	0.65	44	21	34	45	21	34
Rae3	*0.63*	*0.60*	*0.51*	*0.47*	*0.55*	*0.54*	*48*	*27*	*25*	*56*	*29*	*14*
Rae5	0.61	0.74	0.78	0.64	0.67	0.67	46	18	36	44	19	36
Wittenoom												
*Wal1**	*0.58*	*0.50*	*0.56*	*0.33*	*0.46*	*0.51*	*35*	*36*	*29*	*37*	*37*	*25*
Rae4	*0.45*	*0.53*	*0.51*	*0.55*	*0.56*	*0.61*	*37*	*28*	*35*	*38*	*27*	*35*
Mam3*	0.43	0.49	0.50	0.55	0.62	0.63	46	22	31	47	25	27
Mam2	0.54	0.56	0.62	0.53	0.56	0.58	43	21	36	63	17	20
Mam1	0.48	0.51	0.53	0.47	0.52	0.54	47	21	32	60	19	20
Fortescue Group												
Roy1	0.58	0.62	0.64	0.54	0.60	0.58	50	18	31	57	19	24
Roy10	0.56	0.64	0.64	0.53	0.58	0.60	55	17	27	60	19	21
Roy2	0.72	0.78	0.77	0.59	0.65	0.63	56	18	26	58	20	21
Roy11	0.57	0.57	0.65	0.54	0.57	0.65	54	17	30	60	19	21
Roy3	0.56	0.60	0.57	0.53	0.57	0.57	52	20	29	59	20	21
War5	0.59	0.63	0.68	0.56	0.60	0.61	53	17	30	62	18	20
*War1**	*0.46*	*0.50*	*0.46*	*0.43*	*0.49*	*0.46*	*46*	*21*	*34*	*51*	*22*	*27*
*Mad1**	*0.48*	*0.48*	*0.30*	*0.43*	*0.51*	*0.36*	*38*	*23*	*39*	*48*	*26*	*25*
Har1	0.61	0.77	0.69	0.54	0.57	0.60	57	18	25	57	22	21
FVG1	0.49	0.51	0.54	0.46	0.50	0.51	46	18	36	49	20	31
FVG2	0.47	0.51	0.52	0.46	0.51	0.53	42	27	32	46	28	26
War2	*0.46*	*0.50*	*0.41*	*0.38*	*0.46*	*0.41*	*41*	*25*	*34*	*48*	*27*	*25*
Tum1	*0.43*	*0.45*	*0.44*	*0.43*	*0.54*	*0.54*	*44*	*21*	*35*	*50*	*25*	*26*

The **Mt McRae Shale** has an average thickness of 50 m. The lower 15 m contain massive, highly kerogenous black shale interbedded with chert, with the pyrite content increasing upwards (Harmsworth et al., 1990). The middle 10 to 15 m of alternating chert and kerogenous shale are highly pyritic, with nodules up to 2 cm in diameter. The unit terminates with two bands up to 20 cm thick of almost massive pyrite overlain by ~10 m of non-pyritic black shale and several meters of BIF and ferruginous chert interbedded with shale. The massive to plane laminated black shales of the Mt McRae Shale (*Bee1, Rae1–Rae6*) are generally very fine grained and have varying contents of kerogen, quartz, muscovite, illite, chlorite, dolomite, pyrite, hematite and magnetite. They probably had a distal northerly source, but it is currently unclear whether the clastic material was volcanic or terrigenous (Morris, 1993). However, the depositional environment might have been hemipelagic. The Mt McRae Shale grades into the overlying Brockman Iron Formation as BIF contents increase (Harmsworth et al., 1990).

The **Brockman Iron Formation** consists of several hundred meters (620 m at Tom Price and 500 m at Newman) of alternating BIF, chert, shale, dolomite and fine tuff (Harmsworth et al., 1990). Deposition occurred at ~2.47 Ga on a clastic-starved open platform or shelf with normal open oceanic circulation. BIF was probably precipitated in a gradually subsiding back-arc continental setting (Blake and Barley, 1992). The Brockman Iron Formation has been subdivided into four members. The lowermost *Dales Gorge Member*, with an approximate thickness of 150 m, consists of seventeen cycles called 'S-macrobands'. They contain oxide facies BIF (*Dal2*) alternating with shale, chert, carbonate and silicate BIF. The S-macrobands may have formed when the continuous silica and iron precipitation was modified by episodes of increased pyroclastic input (Morris, 1993). The S-macrobands comprise 40 to 45% shale (*Dal1*) in layers ranging from a few centimeters to up to 2 m. The gray or green shales are very fine grained and massive with varying concentrations of kerogen. They predomi-

Table A3. Ratios and maturity parameters based on aromatic hydrocarbons,[a] and methyladamantane and methyldiamantane indices.

	TA/ (TA + MA)[b]	TA-I/ (TA-I + II)[c]	DNR-1	TNR	TNR-2	MPI-1	MPR	MPDF	DPR	MDR
Hamersley Group										
Tom Price area										
Dal1	>90%[f]	>90%[g]	6.6	—	—	0.14	1.3	0.49	0.29	5.0
Dal2	—	—	1.3	2.2	1.3	0.68	1.7	0.54	0.45	1.6
Rae1	>95%[f]	35%	3.5	0.53	0.58	0.06	1.1	0.44	—	1.4
Rae2	>95%[f]	95%	4.0	0.70	0.62	0.74	1.5	0.46	—	—
Rae6	—	—	13.5	2.4	1.4	0.08	2.2	0.60	0.25	8.6
Bee1	93%	78%	3.7	1.2	0.72	0.10	1.5	0.52	0.18	1.7
Mt Whaleback Mine										
Wal2	—	—	5.3	0.72	0.57	—	—	—	—	0.50
Rae3	—	—	4.2	—	—	—	—	—	—	—
Rae5	—	—	4.2	—	—	—	—	—	—	—
Wittenoom area										
Mam3	>95%[f]	85%	—	—	—	0.72	1.3	0.46	0.23	3.0
Mam2	85%	96%	10.0	1.4	0.93	0.67	1.24	0.50	0.20	0.92
Mam1	80%	92%	10.8	2.5	1.3	0.76	1.2	0.49	0.24	1.8
Fortescue Group										
Roy1	92%	94%	5.8	1.2	0.76	0.71	0.87	0.44	0.19	1.0
Roy10	95%	96%	6.3	0.71	0.67	—	—	—	0.13	1.1
Roy2	82%	96%	—	—	—	—	—	—	—	—
Roy11	80%	95%	5.4	0.63	0.60	—	—	—	—	—
Roy3	77%	96%	6.8	1.3	0.85	0.73	1.2	0.47	—	1.3
War5	97%	98%	6.8	1.0	0.79	—	—	—	—	0.74
Har1	>95%[f]	98%	8.6	0.81	0.83	0.84	1.1	0.48	0.18	0.93
FVG1	88%	59%	6.8	1.2	0.90	0.82	1.3	0.49	0.24	1.1
FVG2	>90%[f]	51%	7.9	1.1	0.82	0.69	1.4	0.55	0.27	2.2
Tum1	>95%[f]	76%	12.6	3.1	1.7	0.46	1.9	0.61	0.36	1.7
Diesel[h]	—	—	6.5	1.0	0.86	1.2	1.8	0.59	0.82	3.7

[a] Concentrations were determined by corrected GC-MS signal areas of the molecular ion in the SIR or full scan mode. Compound abbreviations: Naph = naphthalene; MN = methylnaphthalene; DMN = dimethylnaphthalene; TMN = trimethylnaphthalene; Phen = phenanthrene; MP = methylphenanthrene; DMP = dimethylphenanthrene; DBT = dibenzothiophene; MDBT = methyldibenzothiophene; PhN = phenylnaphthalene. Aromatic parameters are based on absolute compound concentrations and are defined as follows: **DNR-1** = (2,6-DMN + 2,7-DMN)/(1,5-DMN); **DNR-6** = (2,6-DMN + 2,7-DMN)/(1,4-DMN + 2,3-DMN); **TNR** = 2,3,6-TMN / (1,3,5-TMN + 1,4,6-TMN); **TNR-2** = (1,3,7-TMN + 2,3,6-TMN)/(1,3,5-TMN + 1,3,6-TMN + 1,4,6-TMN); **MPI-1** = 1.5 × (2-MP + 3-MP)/(Phen + 1-MP + 9-MP); **MPR** = 2-MP/1-MP; **MPDF** (Methylphenanthrene Distribution Factor) = (3-MP + 2-MP)/(3-MP + 2-MP + 9-MP + 1-MP); **DPR** = (2,6-DMP + 2,7-DMP + 3,5-DMP)/ (1,3-DMP + 1,6-DMP + 2,5-DMP + 2,9-DMP + 2,10-DMP + 3,9-DMP + 3,10-DMP); **MDR** = 4-MDBT/1-MDBT. **PAH/MePAH** ratios (Naph/MN; Biph/MeBP etc.) determined using absolute concentrations of the parent compound and the sum of all methylated isomers.
[b] Triaromatic steroids were measured by GC-MS (SIR) monitoring m/z = 231, and monoaromatic steroids monitoring m/z = 253. Peak areas are uncorrected. **TA/(TA + MA):** TA (triaromatic steroids) = C_{20}-TA + C_{21}-TA + Σ (C_{26} to C_{28}-TA 20[S + R]); MA (monoaromatic steroids) = C_{21}-MA + C_{22}-MA; higher monoaromatic steroids were not included in this ratio as they were below detection limit in most samples.
[c] **TA-I/(TA-I + II)** = (C_{20}-TA + C_{21}-TA)/(C_{20}-TA + C_{21}-TA + Σ (C_{26} to C_{28}-TA 20 [S + R])).
[d] Relative methyladamantane and methyldiamantane concentrations were determined by GC-MS in SIR mode using uncorrected signals m/z = 135 and 187, respectively. Methyladamantane Index **MAI** = 1-MA/(1-MA + 2-MA); MA = methyladamantane. Methyldiamantane Index **MDI** = 4-MD/(1-MD + 3-MD + 4-MD); MD = methyldiamantane. Values in italics might be affected by coeluting signals.
[e] '—' = not detectable; ((= not measured.
[f] Monoaromatic steroids were below detection limit. '>' indicates that the given number is a minimum value.
[g] C_{26+} triaromatic steroids were below detection limit. '>' indicates that the given number is a minimum value.
[h] Mobil, Canberra 29.5.2000.

nantly contain stilpnomelane and chlorite and varying amounts of quartz, feldspars, micas and sulfides. The shales probably formed by a combination of chemical precipitation and volcanic ash fall-out, with clear evidence of a terrigenous clastic contribution lacking (Morris and Horwitz, 1983). The overlying ~50 m thick *Whaleback Member* is like an iron-poor variant of the S-macrobands. It contains alternating bands where shale (*Wal1* and *Wal2*) or BIF and chert is predominant. In comparison to the Dales Gorge Member, shales have higher kerogen contents, less stilpnomelane and contain prominent sulfide-rich layers (Morris, 1993).

	Naph/ MN	BiPh/ MeBP	Fl/ MeFl	DBT/ MDBT	Phen/ MP	MP/ DMP	9MP/ 1MP	1PhN/ 2PhN	MAI[d]	MDI[d]
Hamersley Group										
Tom Price area										
Dal1	0.59	0.60	2.4	2.3	4.9	2.4	1.6	0.1	*88*	—
Dal2	0.70	0.67	0.70	0.15	0.74	0.90	1.3	0.1		
Rae1	3.5	6.4	5.3	4.4	11	1.9	1.9	0.3	*73*	*60*
Rae2	0.51	0.47	—	—	0.49	0.97	2.3	—		
Rae6	2.1	8.3	1.8	8.5	11	8.7	1.7	0.1	95	58
Bee1	4.6	5.9	4.7	3.3	8.0	2.3	1.6	0.2	—	57
Mt Whaleback Mine										
Wal2	1.7	3.0	—	24	>100	High	—	5.9	—	59
Rae3	6.2	3.2	—	—	—	—	—	9.0	97	—
Rae5	7.2	21	—	71	>100	High	—	6.9	70	60
Wittenoom area										
Mam3	0.76	0.52	—	0.18	0.44	0.32	1.5	0.1	[e]	
Mam2	0.09	0.24	—	0.20	0.62	0.62	1.2	2.0		
Mam1	0.07	0.34	0.30	0.29	0.45	0.97	1.3	0.5	*56*	—
Fortescue Group										
Roy1	0.03	0.35	0.24	0.26	0.36	0.64	1.1	4.3	—	*43–61*
Roy10	0.39	0.55	—	0.22	0.35	0.89	—	2.7	—	*52–69*
Roy2	—	—	—	—	—	—	—	—		
Roy11	0.10	0.44	—	—	0.26	0.67	—	4.6		
Roy3	0.01	0.38	—	0.27	0.44	0.93	1.6	—		
War5	0.03	0.28	—	0.18	0.55	0.60	—	3.5		
Har1	0.13	0.22	—	0.20	0.35	0.36	1.1	1.0	58	—
FVG1	0.07	0.32	0.41	0.15	0.39	0.80	1.8	—	76	—
FVG2	0.39	0.51	0.52	0.46	0.72	1.5	1.3	0.7		
Tum1	0.15	0.15	0.41	0.27	1.5	1.6	1.3	0.3	75	—
Diesel[h]	0.12	0.18	0.23	0.25	0.34	1.1	1.3	—		

J. J. Brocks et al.

Table A4. Stable carbon isotopic composition[a] of kerogen and individual hydrocarbons.

	Kerogen	n-C$_{10}$	n-C$_{11}$	n-C$_{12}$	n-C$_{13}$	n-C$_{14}$	n-C$_{15}$	n-C$_{16}$	n-C$_{17}$	n-C$_{18}$	n-C$_{19}$	n-C$_{20}$	n-C$_{21}$	n-C$_{22}$	n-C$_{23}$	n-C$_{24}$	Pr	Ph	Naph	Biph	Phen
Hamersley Group																					
Tom Price area and Mt Whaleback																					
Rae1	–32.2	–27.8	–26.8	–26.6	–27.5	–27.3	–26.3	—	—	—	—	—	—	—	—	—	—	—	—	*–34*	*–35*
Rae2	–32.8																		—	—	—
Bee1[b]	–33.5	–28.0	–26.4	–27.0	–27.7	–27.2	–27.2	–27.5	–27.9	29.0	—	—	—	—	—	—	*–28.7*	*–31.0*	–30.0	–33.0	–31.9
Dal1	–32.0	—	–26.2	–27.2	–27.5	–27.4	–28.8	–29.0	–29.1	–29.8	–29.0	–29 ± 1	–28.7	–27.9	—	—	*–30.3*	*–29.8*			
Rae6[c]																			–30.4	–33.8	
Rae3	–34.6	—	—	—	—	—	—	—	—	—	—	—	—	—	—	—	—	—			
Wittenoom area																					
Mam2	–41.3	–27.6	–27.6	–27.9	–28.7	–28.3	–29.5	–28.8	–29.0	–28.4	–29.0	–30.0	–27.6	—	—	—	*–29.0*	—			
Mam1	–46.8	—	—	–27.8	–26.2	–25.6	–27.0	–26.2	–26.2	–26.5	–26.6	–26.8	–26.9	–26.8	–27.2	—	*–28.8*	*–29.6*			
Fortescue Group																					
Roy1	*–39.5*	—	—	—	–28.0	–27.9	–28.6	–27.0	–26.2	–26.1	–26.9	–26.8	–27.2	–27.6	—	—	*–29.4*	*–29.5*			
Roy10	–40.3	–28.0	–27.5	–27.9	–27.3	–28.1	–29.2	–28.5	–29.1	–28.5	–29.4	–27.4	—	—	—	—	*–29.8*	—			
Roy2	*–39.6*	—	—	—	—	*–28.1*	*–30.9*	–27.4	–26.0	–27.4	–27.1	–27.6	–28.3	—	—	—	*–29.8*	*–30.1*			
Roy11	–41.5	–27.7	–27.6	–27.4	–27.6	–28.3	–28.9	–28.4	–28.5	–28.3	–29.0	–28.7	—	—	—	—	*–30.1*	*–30.6*	—	—	—
Roy3	–41.1	—	–26.4	–27.5	—	–27.3	–29.4	–27.4	–27.0	–26.3	–26.4	–26.2	–26.2	—	—	—	*–28.9*	*–28.8*	—	—	—
War5	–44.6																				
War1	–37.1																				
Har1	–32.9	—	—	–26.0	–26.0	–25.7	–26.0	–25.3	–26.2	–26.1	–26.8	–25.9	—	—	—	—	*–27.2*	*–26.1*			
War2	–47.4																				
Tum1	–46.5	—	—	–28.7	–28.2	—	–28.4	–27.7	–27.2	–27.6	–28.1	–27.5	–27.5	–27.8	—	—	*–28.6*	*–29.1*			
FVG1	–44.1																				
FVG2	–45.6	—	—	—	–28.0	–27.5	–27.3	–27.5	–27.3	–27.7	–28.0	–28.4	–27.3	–26.9	–27.0	–27.6	*–28.3*	*–31.4*			

[a] All carbon isotope values δ^{13}C are vs PDB in ‰ notation; '—' = not measurable; ' ' = not measured. Statistical error ±0.1‰ for kerogen, ±0.4‰ for n-alkanes and acyclic isoprenoids, and ±1‰ for aromatic hydrocarbons. Values in italics are possibly affected by coeluting signals or an uneven baseline, and have an unknown error.

[b] *Bee1*: δ^{13}C (methylnaphthalenes) = –30.9‰; δ^{13}C (dibenzofuran) = –30‰; δ^{13}C (fluorene) = –29‰; δ^{13}C (phenylnaphthalenes) = *–33*‰.

[c] *Rae6*: δ^{13}C (methylnaphthalenes) = –28.8‰; δ^{13}C (dimethylnaphthalenes) = –28‰; δ^{13}C (methylbiphenyls) = –30‰; δ^{13}C (fluorene) = –29‰; δ^{13}C (phenylnaphthalenes) = –33‰.

Table A5. Extract/blank ratios ([compound A in rock extract]/[compound A in procedural blank]) for representative samples and representative biomarkers from the Hamersley and Fortescue Groups.

	Hopanes		Steranes		
	Ts[a]	C_{29}-$\alpha\beta$	C_{27}-$\beta\alpha$-20S	C_{28}-$\alpha\alpha\alpha$-20S	C_{29}-$\alpha\beta\beta$-20 (S + R)
Dal2*	20	36	15	27	18
Rae1	180	200	210	790	710
Rae2	280	610	530	880	1000
Rae6	1	1	1	1	1
Wal2	410	220	370	300	450
Rae3	4	7	12	7	5
Mam3*	80	110	39	36	64
Mam1	540	410	840	720	550
Roy1	1000	980	3100	1400	1300
Roy2	100	170	1200	420	320
Roy3	300	230	820	450	340
Mad1*	6	5	7	11	6
Tum1	23	27	7	7	12

[a] Compound abbreviations are defined in the text.
* Kerogen-free or kerogen-poor 'blank' samples.